

# Can linear stability analyses predict the development of river bed waves with lengths much larger than the water depth?

Hermjan Barneveld<sup>1</sup>, Erik Mosselman<sup>2</sup>, Victor Chavarrias<sup>3</sup>, and A.J.F. (Ton) Hoitink<sup>4</sup>

<sup>1</sup>Wageningen University and Research

<sup>2</sup>Deltares & Delft University of Technology

<sup>3</sup>Unknown

<sup>4</sup>Wageningen University

December 8, 2022

## Abstract

Sustainable river management can be supported by models predicting long-term morphological developments. Even for one-dimensional morphological models, run times can be up to several days for simulations over multiple decades. Alternatively, analytical tools yield metrics that allow estimation of migration celerity and damping of bed waves, which have potential for being used as rapid assessment tools to explore future morphological developments. We evaluate the use of analytical relations based on linear stability analyses of the St. Venant-Exner equations, which apply to bed waves with spatial scales much larger than the water depth. With a one-dimensional numerical morphological model, we assess the validity range of the analytical approach. The comparison shows that the propagation of small bed perturbations is well-described by the analytical approach. For Froude numbers over 0.3, diffusion becomes important and bed perturbation celerities reduce in time. A spatial-mode linear stability analysis predicts an upper limit for the bed perturbation celerity. For longer and higher bed perturbations, the dimensions relative to the water depth and the backwater curve length determine whether the analytical approach yields realistic results. For higher bed wave amplitudes, non-linearity becomes important. For Froude numbers  $> 0.3$ , the celerity of bed waves is increasingly underestimated by the analytical approach. The degree of underestimation is proportional to the ratio of bed wave amplitude to water depth and the Froude number. For Froude numbers exceeding 0.3, the net impact on the celerity depends on the balance between the decrease due to damping and the increase due to non-linear interaction.

# Propagation of bed waves in rivers: analytic approach and comparison to numerical modelling

H.J. Barneveld<sup>1,4</sup>, E. Mosselman<sup>2,3</sup>, V. Chavarrías<sup>2</sup>, A.J.F. Hoitink<sup>1</sup>

<sup>1</sup>Wageningen University and Research, Hydrology and Quantitative Water Management Group,

Department of Environmental Sciences, Droevendaalsesteeg 3, 6708 PB Wageningen, the Netherlands

<sup>2</sup>Deltares, P.O. Box 177, 2600 MH Delft, the Netherlands

<sup>3</sup>Delft University of Technology, Faculty of Civil Engineering and Geosciences, P.O. Box 5, 2600 AA Delft,  
the Netherlands

<sup>4</sup>HKV, Botter 11-29, 8232 JN Lelystad, the Netherlands

## Key Points:

- Rapid assessment metrics from linear stability analysis predict the propagation of small bed waves if  $Fr \leq 0.3$
- For  $Fr > 0.3$  bed waves are more diffusive and propagate slower in time than what follows from linear stability analysis
- Numerical modelling can validate results of linear stability analyses, and vice versa

---

Corresponding author: Hermjan Barneveld, [hermjan.barneveld@wur.nl](mailto:hermjan.barneveld@wur.nl)

## Abstract

Sustainable river management can be supported by models predicting the long-term morphological development. Even for one-dimensional morphological models, run-times can be up to several days for simulations over multiple decades. Alternatively, analytical tools yield metrics for propagation and damping of sediment waves, which might be used as rapid assessment tools for future morphological development. Here, we present a linear stability analysis of the St. Venant-Exner equations and derive such an analytical relation. With a one-dimensional morphological model we assess the validity range of the analytical approach. The comparison shows that the propagation of infinitesimal bed perturbations is well-described by the metrics that proceed from the linear stability analysis. For Froude numbers over 0.3, diffusion becomes important and the celerity of bed perturbations reduces in time. The linear stability analysis thus provides an upper limit for the celerity of bed perturbations. For longer and higher bed perturbations, the dimensions with respect to water depth and the length of the backwater curve determine whether the analytical approach yields realistic results. It is shown that for higher bed wave amplitudes, non-linearity becomes important. The celerity of bed waves is then increasingly underestimated by the analytical approach, for Froude numbers  $\leq 0.3$ . The degree of overestimation is proportional to the relative amplitude (ratio of amplitude to water depth) of the sediment wave and the Froude number. For Froude numbers exceeding 0.3, the net impact on the celerity depends on the balance between decrease due to damping and the increase due to non-linearity.

## Plain Language Summary

The riverbed responds to climate change and human interventions such as river engineering works and dredging. A pit resulting from sand mining, for example, typically moves in downstream direction through the river, like a wave in the bed elevation. These waves move much slower compared to water waves. This is why works like groynes and embankments in the Rhine and Meuse Rivers, still cause river bed erosion, and this will continue for the next centuries. For proper river management, understanding the development of the riverbed over shorter and longer time scales is paramount. Numerical models are often used to simulate these changes, but these simulations can be long-lasting. Therefore, more efficient alternatives are of interest. In this paper, we developed a theoretical approach to assess the propagation of sediment waves from a simple equation. The simple tool has been compared to numerical model runs. The tool shows to be valid for small sediment waves and river reaches with gentle bed slopes. When bed slopes increase, the approach overestimates the propagation of small sediment waves. For the Dutch Meuse River, the approach is promising for the mildly sloped Sand Meuse, but overestimates bed wave celerities for the upstream steeper Border Meuse.

## 1 Introduction

In lowland rivers, bed morphological processes are generally much slower than hydrodynamic processes. Growth, propagation and damping of bed forms such as ripples and dunes and the development of local erosion pits are examples of short-term morphological processes, taking place on time scales of hours and days. Flood events, variation in sediment supply, and irregularities in river geometry initiate erosion and sedimentation processes, which will develop over longer time scales and longer reaches. Typically, the morphological changes develop over a period of years to centuries, referred to as the engineering time scale. The engineering time-scale is relevant from a perspective of operational river management, typically focused on navigability, flood prevention and nature conservation. In the long term, the river bed may develop towards a (quasi) equilibrium situation. De Vries (1975) introduced a morphological time scale for the development of longitudinal riverbed profiles. He and others e.g. Dade and Friend (1998), Church

and Ferguson (2015)) showed that larger lowland rivers may take  $10^3$  to  $10^5$  years to adapt to permanent changes, for example at the downstream boundary. Here, we focus on the engineering time scale of morphological changes, i.e. the coming century, and aim to develop a rapid assessment tool for predicting these changes.

Numerical models are a valuable tool for predicting morphological changes in river systems. For assessment of the long-term (quasi-) equilibrium situation efficient techniques are available. Arkesteijn et al. (2019) developed a method to predict the quasi-equilibrium channel geometry in the backwater region of a river, as well as its dynamics. The method is efficient, as the transient phase does not have to be computed. At engineering time scales, the initial development of sediment transport and bed level change is particularly relevant, which cannot be readily inferred from an equilibrium. The runtime of numerical morphological models simulating the initial response at engineering timescales is still long. Even for one-dimensional models, where parameters and variables are averaged over the cross-section, a single simulation for a river reach of a hundred kilometres and several decades may take hours or even days. To address uncertainty model input and to evaluate the consequences of the climate change projections, multiple simulations are required, adopting a stochastic or probabilistic approach (e.g. Van Vuren et al. (2005)). Many techniques are being developed to speed up morphological simulations. Besides improvement of numerical solvers, efforts to improve model efficiency are focused on the development of a morphological acceleration factor (e.g. Lesser et al. (2004), Carraro et al. (2018)), simplification of governing equations (e.g. the quasi-steady approach, first introduced by De Vries (1965)), and reduction of spin-up time (e.g. Yossef et al., 2008).

Analytical solutions offer an alternative for numerical simulation of propagation and damping of disturbances of the river bed. A linear stability analysis provides solutions for celerity and damping of infinitesimal perturbations in the flow and at the river bed. Grijzen and Vreugdenhil (1976) and Ponce and Simons (1977) performed such analyses, starting from perturbations in the flow. De Vries (1965) derived characteristic celerities of flow and river bed disturbances, and Vreugdenhil (1982) performed a linear stability analysis of the equations for flow and sediment, assuming quasi-steady circumstances, which simplifies the analysis. In the latter case, the time-derivatives in the governing flow equations were neglected, which was justified by De Vries (1965) for small values of the Froude number. Sieben (1996), Lyn and Altinakar (2002) and Lanzoni et al. (2006) elaborated further on linear stability analyses, concentrating on mountain rivers and thus transcritical (Froude number in range 0.8-1.2) and supercritical flow conditions. Lanzoni et al. (2006) also addressed subcritical flow conditions. They performed numerical simulations to check the character of the analytical expressions for celerities of infinitesimal flow and sediment waves, without performing a comprehensive comparison between analytical and numerical results. They found that the results of the linear stability analyses, in terms of direction of propagation (upstream, downstream) and amplification or damping of perturbations, agree with numerical simulations.

The analytical solutions clearly provide insight into the physics of hydraulic and morphological processes, but it remains unknown to what extent the relations can be applied for practical applications in lowland rivers, where perturbations are not infinitesimally small. In this paper a linear stability analysis is performed for the complete set of one-dimensional flow and sediment equations, which differs slightly from previous studies in that the length of the perturbations is a parameter. The analysis, based on linearisation of the terms in the governing equations, provides relations for celerity and damping of flow and sediment waves. We test a solution that is consistent with the spatial-mode analysis of Grijzen and Vreugdenhil (1976), which differs from the temporal-mode analysis adopted by for example Lanzoni et al. (2006). The analysis shows that the governing parameters agree with the other analyses, namely the Froude number, the degree of unsteadiness, the strength of bed friction, and the sediment load. We validate the re-

sulting metric for celerity of sediment waves using a one-dimensional numerical model, performed with infinitesimal perturbations in flow and the river bed. This assures a fair comparison to the analytical results. Additionally, simulations with larger flow and sediment waves have been carried out, to define the range within which the analytical results may be used as a rapid assessment tool for morphological development in lowland rivers.

Section 2 describes the linear stability analysis, providing analytical expressions of celerity and damping. In the same section the numerical model ELV is introduced and the simulations performed are described. Results of the linear stability analysis, the comparison with numerical results and assessment of the validity range of the analytical relations are given in Section 3. Practical application of the results are further elaborated in Section 4.

## 2 Methods

### 2.1 Model Equations

The one-dimensional governing equations describing bed evolution read as:

$$\frac{\partial u}{\partial t} + u \frac{\partial u}{\partial x} + g \frac{\partial h}{\partial x} + g \frac{\partial z}{\partial x} = -g \frac{u^2}{C^2 h} \quad (1)$$

$$\frac{\partial h}{\partial t} + h \frac{\partial u}{\partial x} + u \frac{\partial h}{\partial x} = 0 \quad (2)$$

$$\frac{\partial z}{\partial t} + \frac{\partial s}{\partial x} = 0 \quad (3)$$

$$s = f(u, \text{parameters}) \quad (4)$$

which include the 1D Saint Venant equations for conservation of mass and momentum of water (Eq 1 and Eq 2), the continuity equation for sediment (Eq 3) and a capacity-limited sediment transport predictor (Eq 4). The latter two equations together form the Exner equation. Herein:

$t$  = time (s)

$x$  = longitudinal co-ordinate (m)

$u$  = water velocity averaged in a cross-section (m/s)

$h$  = water depth (m)

$z$  = bed level (m)

$C$  = Chézy coefficient, hydraulic roughness ( $\text{m}^{1/2}/\text{s}$ )

$s$  = sediment transport per unit of width (bulk volume) ( $\text{m}^2/\text{s}$ )

$g$  = acceleration due to gravity ( $\text{m}/\text{s}^2$ )

This set of equations forms the base for the linear stability analysis and the numerical models applied in this study.

### 2.2 Linear Stability Analysis

The theory of linear stability analysis provides insight in the physics of flow and sediment transport, and offers a first approximation of the celerity of propagation and attenuation (or amplification) of bed perturbations. Table 1 presents an overview of existing theoretical one-dimensional analyses of river dynamics and morphodynamics. The differences in existing analyses relate to details of the mathematical problem addressed in the study, and the choice of the normal modes adopted for solving the linearized set

**Table 1.** Overview of existing theoretical 1D analyses of hydrodynamic and morphodynamic model equations. HY = hydrodynamic equations. MO = morphodynamic equations. ODE = ordinary differential equation. PDE = partial differential equations. u/s = upstream. d/s = downstream. Solutions proceed directly from boundary conditions, using a Laplace transform of the PDE, or based on substitution of exponential functions  $\exp(ik_r x - k_i x - i\omega_r t + \omega_i t)$  for an infinitely large domain.

Description	Equations	Substitution of exponential functions				Boundary conditions	References
		$k_r$	$k_i$	$\omega_r$	$\omega_i$		
Backwater effects	HY, ODE	-	-	-	-	d/s+ $\Delta(z+h)$	Bélanger (1828)
Flood propagation with temporal damping	HY, PDE	$2\pi/L$	0	$2\pi c/L$	$-4\pi^2 D/L^2$	-	Ponce and Simons (1977)
Flood propagation with spatial damping	HY, PDE	$2\pi/L$	$1/L_D$	$2\pi c/L$	0	-	Grijns and Vreugdenhil (1976)
Propagation of infinitesimal perturbations	MO, PDE	$2\pi/L$	0	$2\pi c/L$	0	-	De Vries (1965), De Vries (1966)
Morphodynamic wave and diffusion character	MO, PDE	$2\pi/L$	0	$2\pi c/L$	$-4\pi^2 D/L^2$	-	Vreugdenhil (1982), Lanzoni et al. (2006)
Response to downstream water level	MO, PDE	-	-	-	-	d/s+ $\Delta(z+h)$	De Vries (1973), De Vries (1975)
Aggradation due to sediment overloading	MO, PDE	-	-	-	-	u/s+ $\Delta s$	Ribberink and Van der Sande (1985)
Present study	MO, PDE	$2\pi/L$	$1/L_D$	$2\pi c/L$	0	-	-

of equations. Either the wave number  $k$  is assumed complex, or the wave frequency  $\omega$ , which will later in this section be further explained.

Our linear stability analysis starts with assuming small perturbation of water depth, flow velocity and bed level:

$$\begin{aligned} h &= h_o + h' \\ u &= u_o + u' \\ z &= z_o + z' \end{aligned}$$

The subscript  $_o$  indicates the steady uniform reference situation. The superscript  $'$  indicates a small perturbation to the steady uniform reference situation.

Substitution of these expressions for  $h$ ,  $u$  and  $z$  in equations 1 to 4, and combining the equations to a single equation in one of the parameters, yields:

$$\frac{\partial^2 h'}{\partial t^2} + c \frac{\partial^2 h'}{\partial x \partial t} - D \frac{\partial^3 h'}{\partial x^2 \partial t} + M_1 \frac{\partial^3 h'}{\partial t^3} + M_2 \frac{\partial^3 h'}{\partial x \partial t^2} + M_3 \frac{\partial^3 h'}{\partial x^3} = 0 \quad (5)$$

where:

$$\begin{aligned} c &= 1.5u_o \\ D &= \frac{h_o u_o}{2i_o} \left( 1 - F^2 + \frac{1}{h_o} \left. \frac{\partial f(u)}{\partial u} \right|_o \right) \\ D_{11} &= \frac{h_o u_o}{2i_o} (1 - F^2) \\ M_1 &= \frac{u_o}{2gi_o^2} \\ M_2 &= \frac{u_o}{gi_o} \\ M_3 &= -\frac{u_o^2}{2i_o} \left. \frac{\partial f(u)}{\partial u} \right|_o \\ F &= \frac{u}{\sqrt{gh}} \end{aligned}$$

Similar equations can be obtained for  $u'$  and  $z'$ . Equation 5 can be solved analytically by assuming a periodic solution for the water depth of the form:

$$h' = h_o \hat{h} \times e^{i(kx + \omega t)} \quad (6)$$

where:

$$\begin{aligned} h_o &= \text{steady uniform water depth} \\ \hat{h} &= \text{dimensionless depth amplitude function} \\ k &= \text{wave number} \\ \omega &= \text{frequency} \\ i &= \sqrt{-1} \end{aligned}$$

Two approaches can be adopted to obtain a solution for the perturbed variables (Drazin & Reid, 2004), a temporal mode analysis and a spatial mode analysis. In the temporal mode analysis, the frequency  $\omega$  is assumed complex and the real part of the wave number is assumed to be equal to  $k_r = \frac{2\pi}{L}$ , where  $L$  is the wave length. In the spatial mode analysis, the wave number  $k$  is assumed complex and the wave frequency  $\omega$  real, as in  $\omega_r = \frac{2\pi}{T}$ , where  $T$  is the wave period. The complex roots, i.e. either  $\omega$  or  $k$ , determine the propagation and damping of perturbations in the flow and at the river bed.

Many of the studies in Table 1 adopted the temporal mode in the analysis, assuming the perturbation wave number real ( $k_r = \frac{2\pi}{L}$ ). Drazin and Reid (2004) describe that the physical properties of spatial modes are closer to the instability phenomena observed in most experiments on parallel flow, compared to temporal modes. In this study we extend the spatial-mode analysis by Grijzen and Vreugdenhil (1976). The corresponding waves proceeding from a spatial mode analysis can be pragmatically interpreted as boundary conditions, which are important in engineering practice. Strictly speaking, however, this type of linear analysis does not build on boundary conditions, but rather on a solution in the time-space domain. The choice of the period of the upstream boundary condition, e.g. the flow time series, sets the wave length of bed perturbation in the river, which is further elaborated in Section 2.3.4. The solution (Eq 6), with known period of the wave  $T$  and thus the value of  $\omega_r$ , represents the shape of the boundary condition.

Our approach allows for a justified comparison between the results of the linear stability analysis and numerical simulations with a discharge time series at the upstream boundary and a bed perturbation as initial condition across the 1D model domain.

In the spatial mode analysis the wave number  $k$  is complex

$$k = k_r + ik_i \quad (7)$$

where  $k_r$  determines the celerity  $c$  of the water and sediment waves,

$$c = -\frac{\omega}{k_r} \quad (8)$$

where  $k_i$  determines the damping of water and sediment waves and

$$L_d = \frac{1}{k_i} \quad (9)$$

$L_d$  is called the relaxation length over which the amplitude of a wave is damped by a factor  $e^{-1}$ .  $c$  and  $L_d$  are the characteristic wave properties.

For convenience, the wave number is first made dimensionless.

$$\hat{k} = \hat{k}_r + i\hat{k}_i = kx_o[-] \quad (10)$$

in which the characteristic length scale  $x_o$  is defined as

$$x_o = \frac{Q_o T}{B_o h_o} = u_o T = \text{a characteristic length scale} \quad (11)$$

Herein,  $Q_o$  is the undisturbed flow and  $B_o$  the undisturbed width. Substitution of Eq (10) and the solution, Eq (6), in Eq (5) leads to a third-order differential equation in the dimensionless wave number  $k$ .

$$\frac{\Psi}{2\pi F^3 E}(\hat{k})^3 + \frac{1}{F^3 E}(1 - F^2 + \Psi)(\hat{k})^2 - \frac{4\pi}{FE}\hat{k} + 3i\hat{k} - \frac{4\pi^2}{FE} + 4\pi i = 0 \quad (12)$$

with three governing parameters,  $F$ ,  $\Psi$  and  $E$ :

$$\Psi = n \frac{s_o}{q_o} = \quad \text{dimensionless transport parameter} \quad (13)$$

$$E = \sqrt{\frac{g^3 T^2}{C^4 h}} \quad (14)$$

Herein,  $n$  is the power in the sediment transport relation  $s = m u^n$ . The parameter  $E$  describes the influence of unsteadiness and non-uniformity. Grijzen and Vreugdenhil (1976) introduced this parameter in their analysis of the flow equations and they defined typical values of  $E$ . For tidal waves,  $E$  takes a value of about  $10^2$  and for flood waves,  $E \approx 10^3 - 5 \cdot 10^4$ .

The solution of equation (12) consists of three roots for  $\hat{k}$ . These roots determine the characteristic wave properties (celerity and damping) of both water and sediment waves.

$$c = -\frac{2\pi u_o}{\hat{k}_r} \quad (15)$$

$$L_d = \frac{u_o T}{\hat{k}_i} \quad (16)$$

## 2.3 Numerical Model Simulations

### 2.3.1 Introduction

To assess the applicability of the results of the linear stability analysis, numerical model simulations are performed. As the linear stability analysis is based on infinitesimal perturbations, numerical simulations with such perturbations should agree with the theoretical results, at least for the initial values. Simulations with non-infinitesimal perturbations and on longer time scales may or may not agree with results from the linear stability analysis, which is here being verified.

### 2.3.2 Model Description

The numerical modelling code ELV is selected (Chavarrias et al., 2019), which is a Matlab code for modelling morphodynamic processes on a one-dimensional domain. ELV solves the full set of equations (1 to 4) in an uncoupled way, with an implicit Preissmann scheme for flow and a first-order forward Euler upwind scheme for morphology. This is called the unsteady model. The model can readily be used to test simplified models, in which terms in the equations are neglected.

### 2.3.3 Model Set-Up

For performing simulations that can be compared to results from the linear stability analysis, a one-branch model was constructed with characteristics as in Table 2.

The branch length was chosen long enough to prevent any impact of the model boundaries on the area of interest, i.e. the area where a bed perturbation propagates and dampens. It was chosen short enough to allow for reasonable simulation times, for a simulation period of 1 to 3 years. The smallest space step, for the simulations with infinitesimal bed perturbations, amounted to 2.5 m (see below). For these simulations with a duration of 1 year, a branch length of 10 km was selected. For simulations with larger bed



**Table 2.** Model set-up for simulation with ELV

Characteristic	Value/description
Model length	10-25 km
Width channel (no floodplains) $B$	100 m
hydraulic roughness, Chézy-value $C$	$40 \text{ m}^{1/2}\text{s}^{-1}$
bed slope $i_b$	0.0001 to 0.0022
space step $\Delta x$	2.5-25 m
time step $\Delta t$	1-5 sec
sediment transport $s$	uniform sediment, transport predictor of Engelund-Hansen (Engelund & Hansen, 1967)
grain diameter $D_{50}$	0.002 to 0.35 m
upstream boundary conditions	time series for discharge and equilibrium sediment transport
downstream boundary condition	uniform flow conditions (stage-discharge relation for uniform flow)

perturbations, the space step could be enlarged. A branch length of 25 km was selected for 3-year period simulations. For exact comparison with the linear stability analysis results, a simple rectangular cross-section with fixed width was adopted. The width of 100 m was selected arbitrarily. A constant Chézy value of  $40 \text{ m}^{1/2}/\text{s}$  was adopted.

The Froude number  $F$  is a key parameter in the linear stability analysis. In this study, we focus on rivers with Froude numbers for which decoupling of the equations for flow and sediment is possible in numerical simulations. De Vries (1973), Morris and Williams (1996), Sieben (1996), Sieben (1999) and Cui et al. (2005), show that this is possible if Froude numbers are smaller than 0.7 to 0.8. In this study, we selected the range of  $F$  between 0.1 and 0.6. With the selected Chézy value ( $C$ ) the corresponding range in bed slope  $i_b$  is between 0.0001 and 0.0022. To select the space step, a sensitivity analysis was carried out for the model with a length of 25 km and a bed perturbation of 1 km long. Simulations were carried out for Froude numbers of 0.4 and 0.6. The space step was reduced from 100 to 50, 25 and 12.5 m. The time step was reduced accordingly, maintaining the Courant–Friedrichs–Lewy or CFL-condition below 1, so as to have sufficient numerical accuracy of the simulations. The analysis showed that the difference between a spatial step of 25 m and 12.5 m was negligible, so 25 m was small enough. A second criterion was to schematize the bed perturbation with at least 20 grid points. With the simulations performed the minimum selected space step was therefore 2.5 m.

In the theoretical analysis, the sediment transport and its non-linearity, expressed with the parameter  $n$ , are important. To have a fair comparison between theory and numerical simulations, we selected a sediment transport predictor with an unequivocal value of  $n$ . The sediment transport predictor of Engelund-Hansen with  $n=5$  was selected for this (Engelund & Hansen, 1967). This formula for total sediment transport does not account for a threshold of motion and is widely used for sand-bed rivers. To ease the comparison between results of the linear stability analysis and numerical modelling results, we use identical sediment transport formulas for all computations. Therefore it was decided to apply the Engelund-Hansen transport predictor also for high Froude numbers and coarse bed material.

For subcritical flow conditions, conditions are needed at the upstream boundary for flow and sediment transport. As the objective of the simulations is to simulate the propagation of sediment waves in the time-space domain, we schematize the sediment wave as a perturbation of the bed. At the upstream boundary, an equilibrium sediment

transport load is imposed, to guarantee a stable river bed in the upstream part of the model. To perturb the flow, a boundary condition is imposed as a base flow, a peak flow and a wave period  $T$ . The linear stability analysis is based on a sinusoidal shape of perturbations, but in our numerical simulations we adopt a more natural shape of the hydrodynamic wave, based on the Dimensionless Unit Hydrograph (DUH) method. By doing so, the application in engineering practices can be better assessed, and we expect that the impact of this choice on the results is negligible. The gamma relation for the DUH method reads (USDA, 2007):

$$\frac{Q}{Q_p} = e^m \left[ \frac{t}{t_p} \right]^m \left[ e^{-m(\frac{t}{t_p})} \right] \quad (17)$$

with:

$Q_p$  = peak discharge

$e$  = constant 2.71183

$m$  = gamma equation shape factor

$\frac{t}{t_p}$  = ratio of the time of DUH coordinate to time to peak of the DUH

With values of  $m$  amounting to 15 and  $t_p$  equal to 20 days, we generate a discharge time series at the upstream boundary with repeating flood waves of an approximate duration of 25 days ( $T$ ), interrupted by periods of approximately 20 days with base flow (Figure 1).

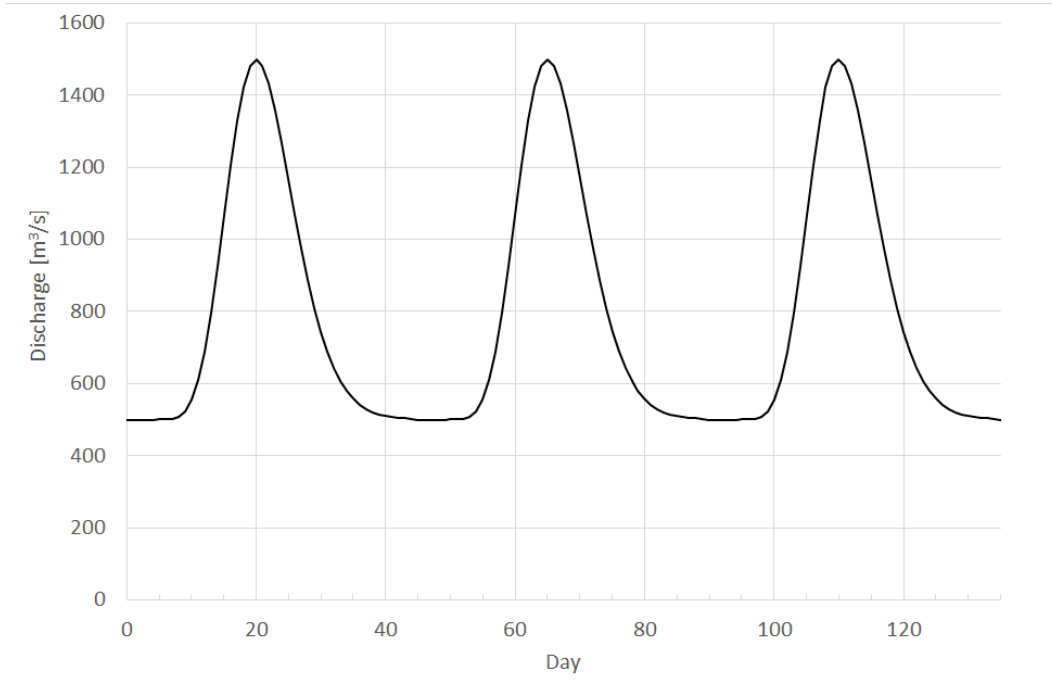


**Figure 1.** sample flood wave boundary condition

The wave period  $T$  of 25 days determines the parameter  $E$  in the governing equation of the linear stability analysis (Eqs. 12 and 14). Depending on the Froude number,  $E$  varies between 15,000 and 30,000 (for  $F=0.6$ ). At the downstream boundary, one condition for the flow is required, for which the water level corresponding to uniform flow is chosen.

### 2.3.4 Performed Simulations

Governing parameters in the linear stability analysis are  $F$ ,  $E$  and  $\Psi$ . We are interested in the validity of the theoretically derived celerities for lowland rivers with Froude numbers up to 0.6 and hydrological conditions and sediment loads characteristic for such environments. The parameter  $E$  is determined by the wave period of the flood wave, which we set at 25 days in a 45 days time domain. For the dimensionless transport parameter  $\Psi$  we adopt a value of  $5 \cdot 10^{-5}$ .

First, we perform numerical simulations with infinitesimal perturbations of the flow and the river bed. We derived consistent combinations of the upstream boundary condition for flow and initial conditions for the bed perturbation. The wave period of the flow boundary condition determines the parameter  $E$ . With selected values of  $F$  and  $\Psi$ , the roots for the dimensionless wave number  $\hat{k}$  (Eq 10) can be determined, providing the celerity of the sediment wave (Eq 15). Eq (8) and  $\omega (= \frac{2\pi}{T})$ , which is known, determine the value of  $k_r$ , which sets the wave length  $L$  of the sediment wave (using  $k_r = \frac{2\pi}{L}$ ). In this way, wave lengths of the bed perturbation of 107 m ( $F=0.1$ ) to 446 m ( $F=0.6$ ) were derived.

To assess the validity of the results of the linear stability analysis for these infinitesimal perturbations at  $t = 0$ , as well as for larger perturbations and for larger time scales (up to 3 years), a more elaborate set of simulations was performed, as summarized in Table 3.

**Table 3.** Numerical simulations performed to validate results from the linear stability analysis.

Set	Qbase (m <sup>3</sup> /s) <sup>a</sup>	Qtop (m <sup>3</sup> /s) <sup>b</sup>	Height (m) <sup>c</sup>	Length (m) <sup>d</sup>	Run duration (yr)	Comment
1	500	505	0.005	matching to flow (107-446 m)	1	base set
2	500	505	0.005	3000	3	long sediment wave
3	500	1500	0.1-0.5	3000	3	large flow and sediment waves

<sup>a</sup>base flow boundary condition

<sup>b</sup>peak flow boundary condition

<sup>c</sup>height bed perturbation / sediment wave

<sup>d</sup>wave length bed perturbation / sediment wave

## 3 Results

### 3.1 Propagation Celerity Inferred From Linear Stability Analysis

The celerity of flow and sediment waves follows from Eq 15. For the sediment waves, the relative celerity is analyzed, which reads:

$$c_{rel} = \frac{c}{u_o} = -\frac{2\pi}{\hat{k}_r} \quad (18)$$

Figure 2 shows the results of this relative celerity for various combinations of  $E$ ,  $F$  and  $\Psi$ . Figure 2 shows that for values of  $\Psi$  equal to or below  $1E-05$ , the results are insensitive to  $E$  when Froude numbers are below 0.6. The results for different values of  $E$  are very similar for these conditions. When sediment transport increases, the parameter  $E$

becomes more important. When  $E$  increases, the relative celerity decreases and may even show a negative tendency, for increasing Froude numbers. This is due to the increasing diffusive character of sediment waves, causing a decrease in the celerity of bed perturbations when Froude numbers increase. This has previously been described by Lisle et al. (2001) and (Lanzoni et al., 2006), and will be further explained in Section 3.2.

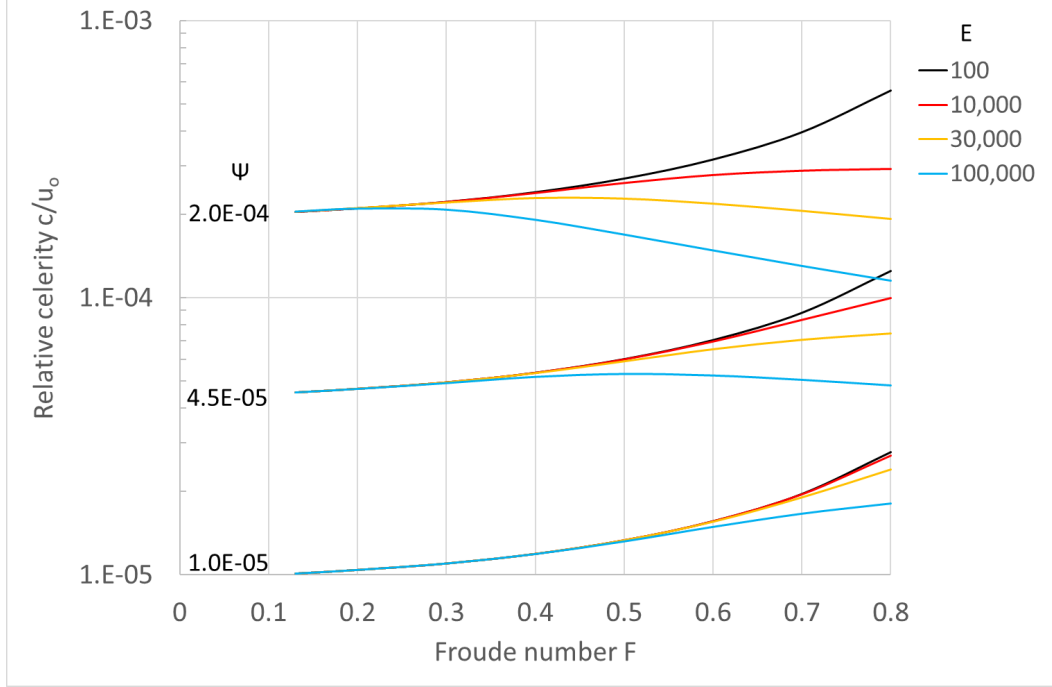


**Figure 2.** Relative celerity of sediment waves in the linear stability analysis.

Figure 3 zooms in on a  $\Psi$  value typical for lowland rivers, such as the River Meuse in the Netherlands. This case is used for the comparison with the numerical results in the next session.

### 3.2 Numerical Modelling Results

From the simulations with a hydraulic upstream boundary condition and initial perturbation of the river bed, the propagation of this bed perturbation was simulated for 3 consecutive periods of 45 days. In each period, a flood wave of 25 days occurred (Figure 1). The period of 45 days was selected by taking the Meuse River in the Netherlands as an example, where the annual sediment transport is known to be mainly concentrated in a period of this duration in the winter season.

Figures 4 and 5 give examples of the propagation of the initial perturbation of the river bed for Froude numbers of 0.2 and 0.6, respectively. The figures show that for  $F=0.2$  the bed perturbation clearly translates in downstream direction, while damping takes place. For  $F=0.6$  translation is small and diffusion of the bed perturbation in time dominates.

The differences in translation for different Froude numbers have been studied further by analyzing the celerity of the bed perturbations during the initial stage of the simulations. Again, a simulation period of 45 days was chosen for this analysis. Results for  $F$  of 0.2 and 0.6 are presented in Figures 6 and 7, respectively, showing the celerity of the crest of a bed perturbation in time. Because of the finite time and space steps, the

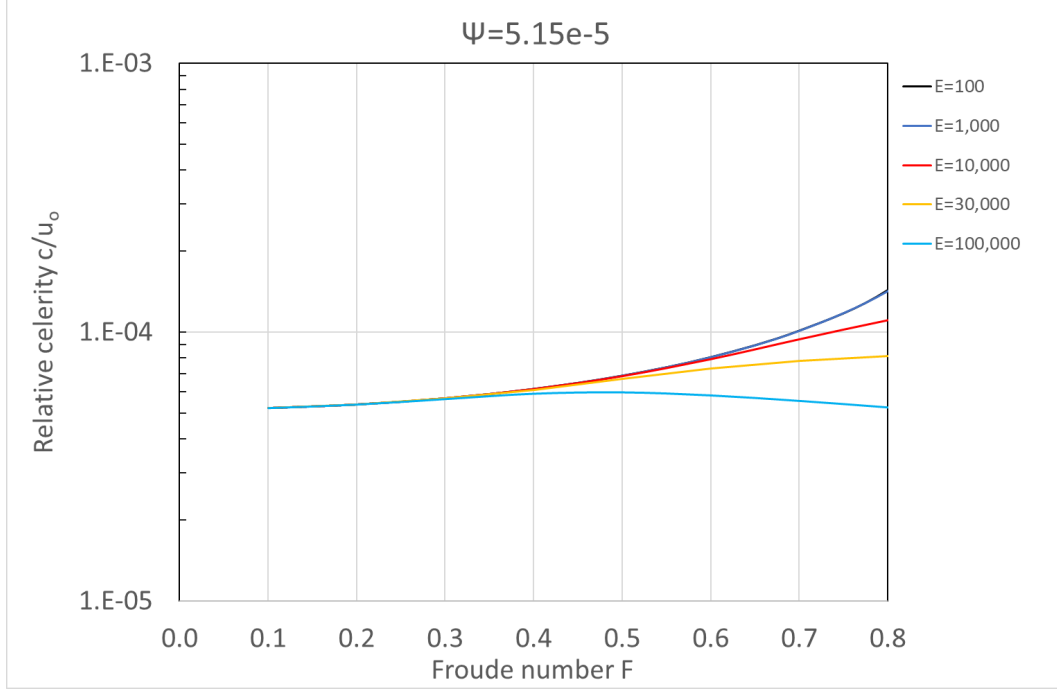


**Figure 3.** Relative celerity of sediment waves in the linear stability analysis for  $\Psi=5.15 \cdot 10^{-5}$

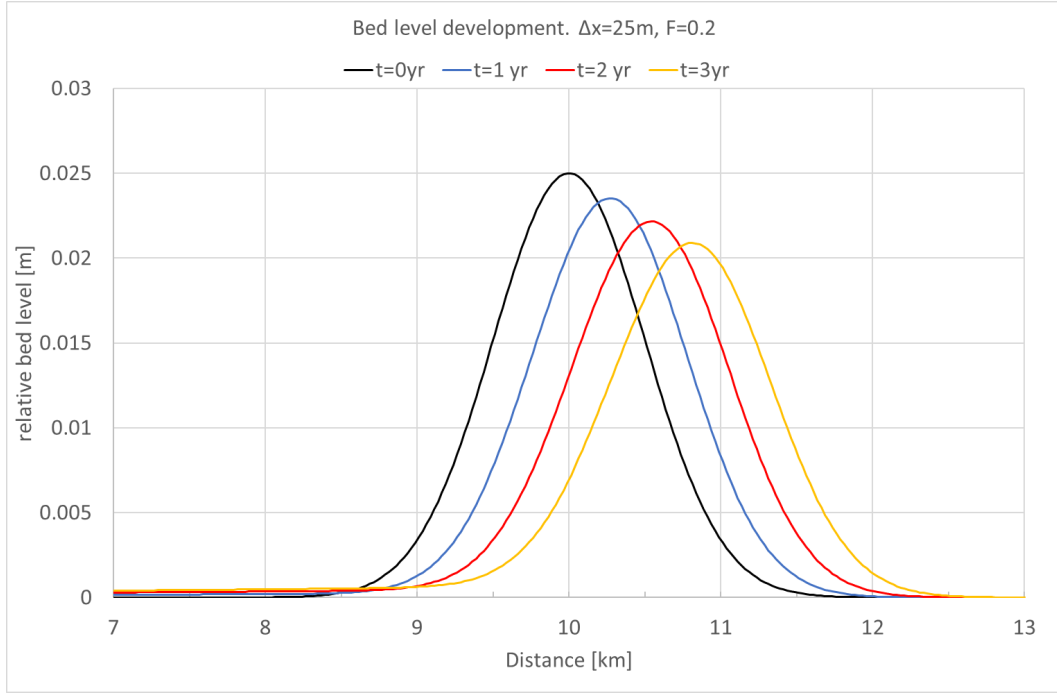


**Figure 4.** Simulated relative bed level (relative to bed slope) of sediment wave for  $F=0.2$

line shows a saw tooth shape. The regression line shows the trend of the celerity. Figure 6 shows that for  $F=0.2$  the bed perturbation propagates at a constant speed. For  $F=0.6$  (Figure 7) the speed of the bed perturbation is initially high, but decreases strongly in the first year.

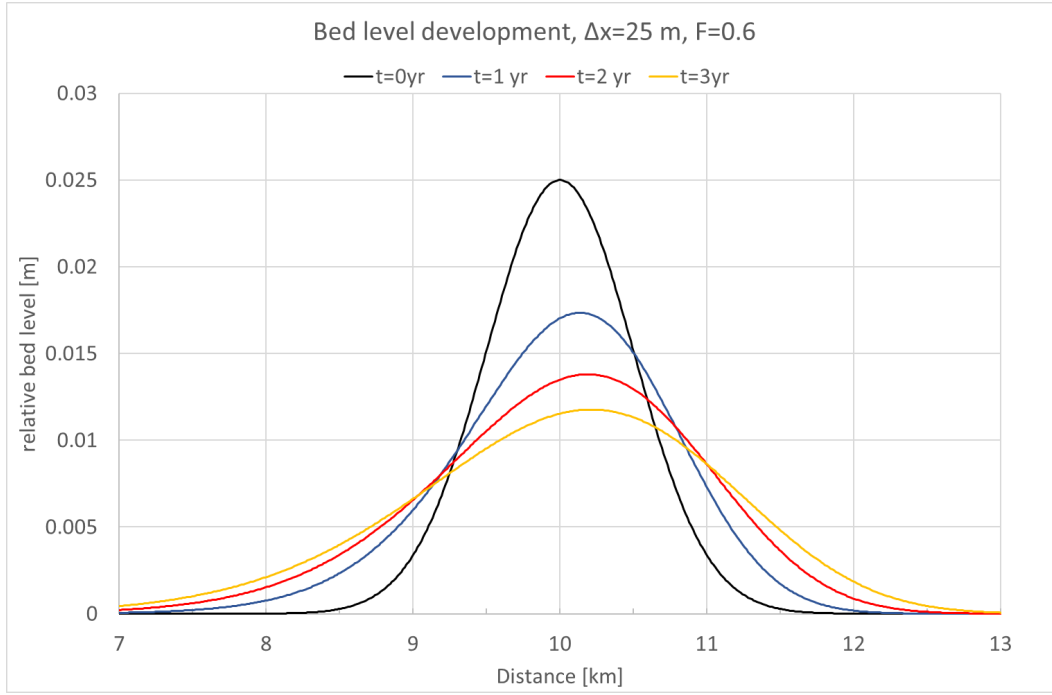


**Figure 5.** Simulated relative bed level (relative to bed slope) of sediment wave for  $F=0.6$ .

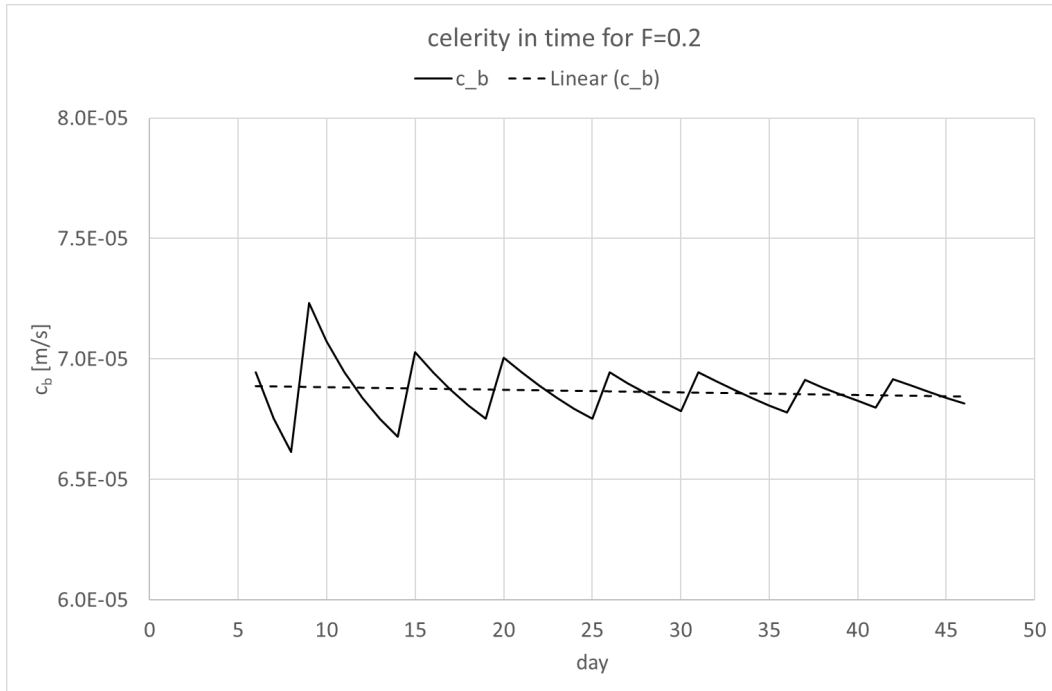


**Figure 6.** Simulated celerity  $c_b$  of the peak of the sediment wave in first year for  $F=0.2$ . The saw-tooth shape of the line is due to the space step in the simulations, providing a shock type development, especially for the first part of the simulation. The regression line shows the stability of the celerity in time.

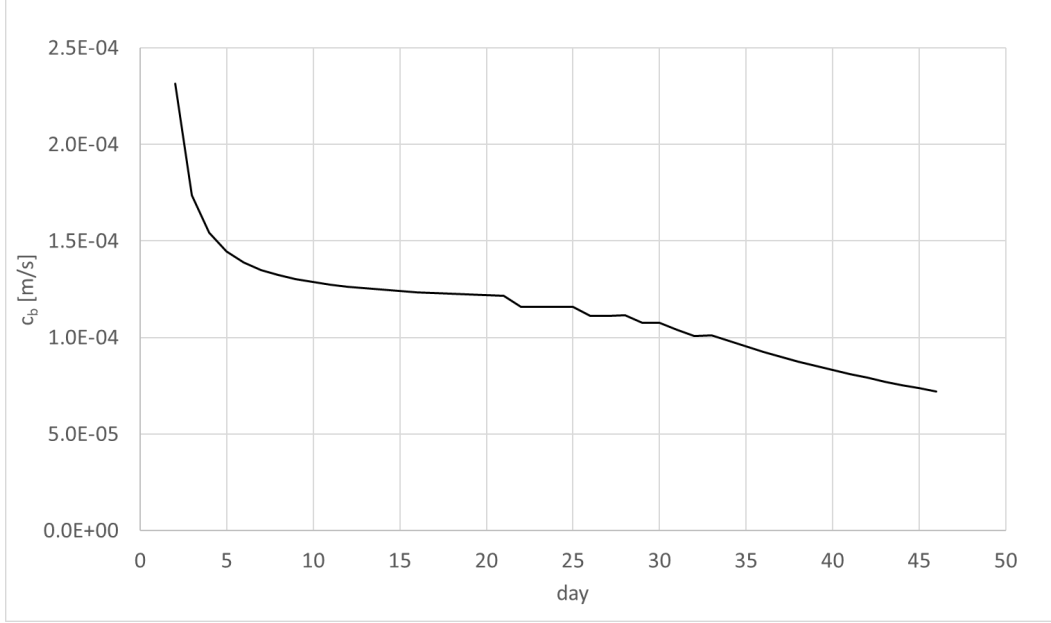


**Figure 7.** Simulated celerity of the peak of the sediment wave in first year for  $F=0.6$ .

Before analysing these findings, the results of the ELV simulations for higher Froude numbers were checked, to avoid that numerical aspects, i.e. numerical diffusion, may explain part of the discrepancy. The simulations for  $F=0.4$  and  $0.6$  were repeated with the one-dimensional numerical model SOBEK-RE (see Ji et al. (2003)). SOBEK-RE has been developed by Deltares in the Netherlands and was validated in various studies and applications. The simulations with SOBEK-RE, with identical boundary conditions, setting of numerical parameters and time and space step, confirmed the diffusive character of bed perturbations for high Froude numbers.

Lisle et al. (2001) studied translation and diffusion for gravel bed rivers. They based their analysis on the Meyer-Peter-Mueller (MPM) bed load transport predictor, but results provide general aspects of wave behaviour for other transport predictors as well. They present the following equation separating terms associated with translation of bed perturbations from those associated with diffusion.

$$\frac{\partial z}{\partial t} = \frac{Kqc_f^{1/2}}{R_s(1-p)} \left[ \frac{\partial z^2}{\partial x^2} + \left( \frac{\partial}{\partial x}(1-F^2) \frac{\partial h}{\partial x} \right) + \dots \right] \quad (19)$$

where  $K$  is an empirical constant in the MPM equation,  $q$  is unit water discharge,  $p$  is the bed porosity and  $R_s$  is the submerged specific gravity of sediment. The unspecified terms in the brackets are non-uniform flow terms, which are small for  $F < 1$ . The first term within the brackets expresses the rate of wave diffusion. The second term expresses the rate of translation. The term  $1-F^2$  clearly indicates that translation decreases with increasing  $F$ . For those cases, diffusion dominates. Physically, this means that diffusion becomes more important when the dimensions of bed perturbations (i.e. height and wave length) become significant compared to the flow characteristics (i.e., the water depth and the length of backwater curve). This explains that for large Froude numbers, with smaller water depth and shorter backwater curves, diffusion of a sediment wave with certain amplitude and wave length is more important than for conditions with small Froude numbers.

Lisle et al. (2001) also refer to a well-documented example for the Navarro River in California in 1995 (Sutherland et al., 2002). Landslide material that entered the steep gravel-bed river (bed slope of 0.0028), formed a sediment wave that dispersed upstream and downstream and mostly disappeared within a few years with no measurable translation.

### 3.3 Comparison between Linear Stability Analysis results and Numerical Simulations

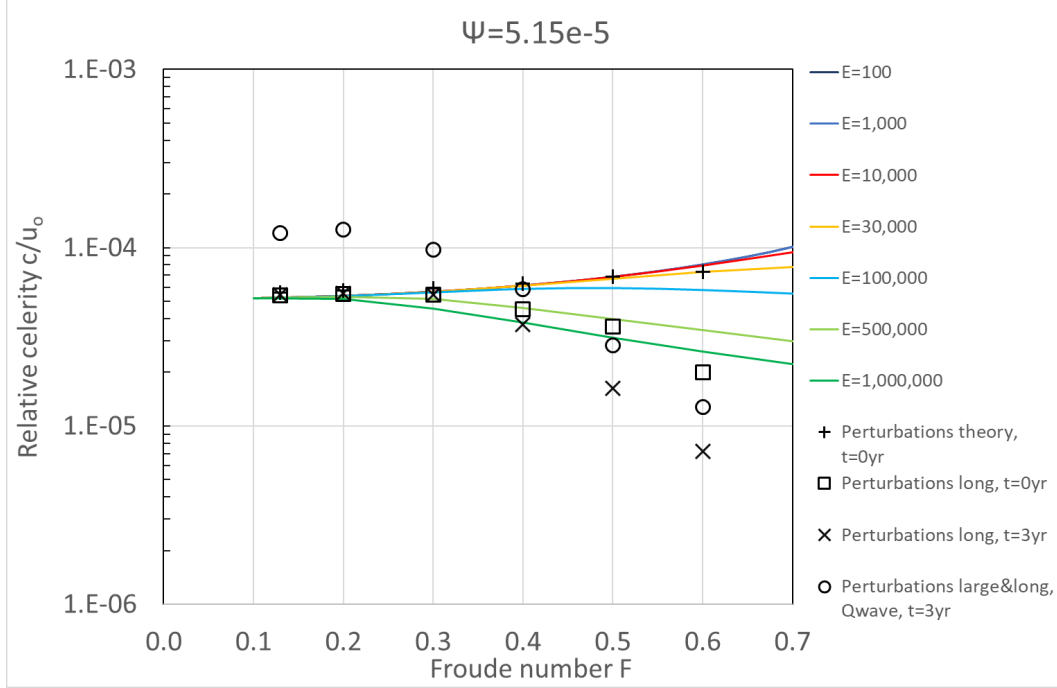


**Figure 8.** Comparison between relative celerity of bed perturbations from linear stability analysis and numerical simulations for  $\Psi=5.15 \cdot 10^{-5}$ .

The results from the numerical simulations are compared with the results from the linear stability analysis in Figure 8. The figure shows that results of the linear stability analysis and numerical simulations agree for infinitesimal perturbations with a wave length coupled to the value of  $E$ , at  $t=0$  (+ markers; Perturbations theory,  $t=0\text{yr}$ ). The numerical results are in good agreement with the area delimited by the lines for  $E=10,000$  ( $F=0.1$ ) and  $E=30,000$  ( $F=0.6$ ). When the wave length of bed perturbations increases to 3,000 m (open box markers; Perturbations long,  $t=0\text{yr}$ ) the simulated initial celerities decrease for Froude numbers of 0.4 and higher. This is due to the increased diffusive character, as explained in the previous section. The linear stability analysis captures this. As already mentioned in Sections 2.2 and 2.3.4, the period of the upstream boundary condition and the wave length of bed perturbation in the river are coupled in the linear stability analysis. This means that the parameter  $E$  and wave length  $L$  are coupled, which is manifest as a relation in Figure 9. For moderate Froude numbers, up to 0.3, this relation is close to linearly increasing. For higher Froude numbers, the increase in parameter  $E$  accelerates with increasing wave length  $L$ .

By choosing a wave length of 3,000 m, the parameter  $E$  increases to 350,000-500,000 for the range of Froude numbers considered. Figure 8 shows that for Froude numbers under 0.3 the impact of longer bed perturbations on the celerity is small, as the depen-



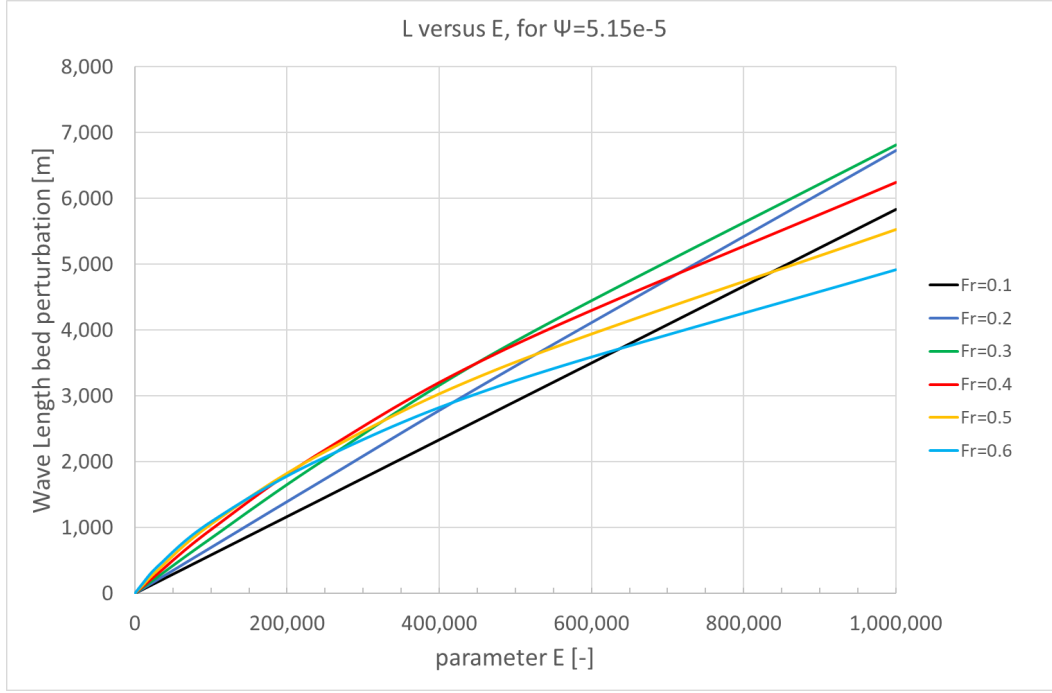


**Figure 9.** Relation between wavelength  $L$  and parameter  $E$  in linear stability analysis for  $\Psi=5.15 \times 10^{-5}$ .

dence on  $E$  shows to be small. The simulated celerities of bed perturbations are fairly constant in time (see Figure 6) and agree with results from the linear stability analysis. For Froude numbers up to and including 0.5, the linear stability analysis still predicts the initial celerities quite accurately when adopting  $E=500,000$ . For even higher Froude numbers, the non-linear effects apparently become more important, and the linear stability analysis overestimates the initial celerities. For Froude numbers of 0.4 and higher the diffusive character is such that the wave length in time increases, and the celerity thus decreases. The celerity from the linear stability is an upper limit, and the deviation from the real celerity increases in time (x markers; Perturbations long,  $t=3$  yr). This slowing down in time is clearly shown in Figure 7.

When the perturbations in the bed are not small (in height and length) and also the flow variations are large, the deviations between linear stability analysis and numerical results further increase. The open circle markers (Perturbations large&long,  $t=3$  yr) in Figure 8 represent simulations with a peak of the flood wave of  $1,500 \text{ m}^3/\text{s}$  (base flow =  $500 \text{ m}^3/\text{s}$ ) and bed waves of 50 cm for  $F=0.1-0.4$  and 10 cm for  $F=0.5-0.6$ . Under those conditions, the relative celerities increase compared to the simulations with small perturbations in bed and flow. This can be explained by the value of  $\Psi$ , which increases when the discharge in the simulations increase. In Figure 9 the simulation results with large perturbations of Figure 8 have been repeated, and results from the linear stability have been added when values of  $\Psi$  are based on the average sediment transports during the simulation (filled circle markers). The increase of values for  $\Psi$  brings results from the linear stability analysis and numerical simulations closer, especially for moderate Froude numbers ( $F=0.1-0.3$ ). However, the relative celerities in this range of Froude numbers are still underestimated by the linear stability analysis. The increased non-linear effects due to the larger perturbations of flow and river bed are responsible for this and (logically) not reproduced by the linear stability analysis. This is further elaborated in the next section and in Figure 12.

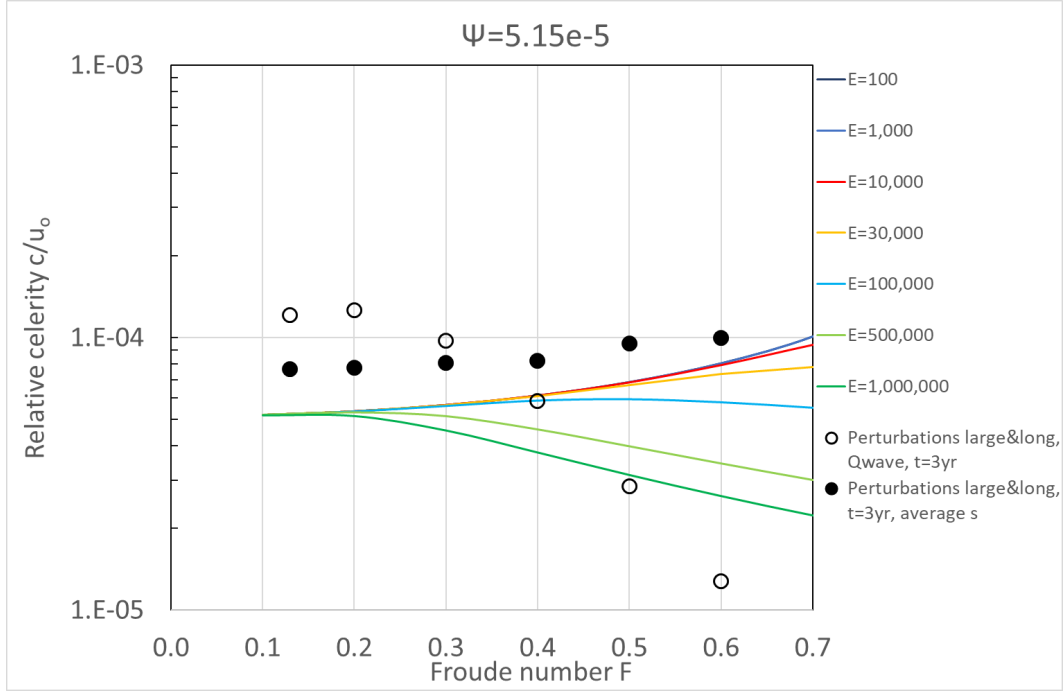


**Figure 10.** Relative celerity of large bed perturbations: linear stability analysis based on initial sediment transport (open circles) and average sediment transport (filled circles). Values of  $\Psi$  increase up to  $7.0\text{--}7.5 \times 10^{-5}$ .

#### 4 Discussion

The predictive value of the analytical approach is large when the diffusive character of sediment waves is small, which appears to be related to the Froude number. For Froude numbers up to 0.3, diffusion of bed perturbations is normally small and celerities derived from the linear stability analysis are representative, even on longer time scales. When dimensions of the bed perturbations increase compared to depth and the backwater length, the diffusive character of sediment waves increases. The linear stability analysis can then still provide a good estimate of the initial celerity of bed perturbations. As the wave length of a bed perturbation grows in time, also the appropriate parameter to be selected in the linear stability analysis changes. The initial choice of the parameters overestimates the celerity of bed perturbations in time when the Froude number exceeds 0.3. The importance of the Froude number and relative dimensions of the bed perturbations confirms results from Lisle et al. (2001) and the theoretical analysis of Vreugdenhil (1982). The diffusion coefficient  $D$ , defined by Vreugdenhil (1982) as  $D = \frac{1}{3} C^2 \Psi h^2 / u$ , the wave number  $k$  and the celerity  $c$  altogether determine how diffusive the system is. Therefore, the Péclet number  $P = cL/D$  (with  $L$  the wave-length) is relevant, which can be considered as the ratio of advection to the rate of diffusion. For high values of  $P$ , the system behaves as a pure diffusion equation and vice versa, as a pure convection equation when  $P$  is small. Of course, the wave length of a convective wave can grow in time and diffusion will increase. The Froude number  $F$  and Péclet number  $P$  are related. For high Froude numbers, backwater curves are short. The wave length of sediment waves thus becomes relatively long, compared to the backwater curve.

Whereas we performed a spatial mode analysis, a temporal mode analysis was briefly elaborated for comparison. In the temporal mode analysis, Equation (12) transforms into an equation for the dimensionless complex frequency  $\hat{\omega}$ .

$$F^2(\hat{\omega})^3 + (2i - 2\hat{L}F^2)(\hat{\omega})^2 + (-3\hat{L}i - (\hat{L})^2(1 - F^2 + \Psi))\hat{\omega} + (\hat{L})^3\Psi = 0 \quad (20)$$

with:

$L$  = wavelength of disturbance

$$L_o = \frac{h_o}{i_o}$$

$$\hat{L} = 2\pi \frac{L_o}{L}$$

$\hat{\omega} = \hat{\omega}_r + i\hat{\omega}_i$  = dimensionless complex frequency

$\hat{\omega}_i$  determines the damping of water and sediment waves.

$\hat{\omega}_r$  determines the celerity of the waves (water and sediment waves)

$$\hat{c} = \frac{c}{u_o} = \frac{\frac{L}{T}}{u_o} = \frac{\hat{\omega}_r}{\hat{k}} \quad (21)$$

Solving Eq 20 again provides the roots determining propagation and damping of disturbances of flow and bed. The character of this equation agrees with the derivation of Lanzoni et al. (2006), see equation 14.

Figure 11 presents the results of the linear stability analyses adopting spatial and temporal modes, compared to the simulated results. Both spatial mode and temporal mode analyses accurately predict the initial celerities of infinitesimal bed perturbations. For longer bed perturbations ( $L=3,000$  m) both approaches are accurate for Froude numbers up to and including  $F=0.3$ . For larger Froude numbers, the spatial mode analysis provides an upper limit for the celerity of bed perturbations. The temporal mode analysis gives somewhat smaller celerities, underestimating the initial celerity, but, similar to the spatial mode analysis, overestimates the celerities for the longer term.

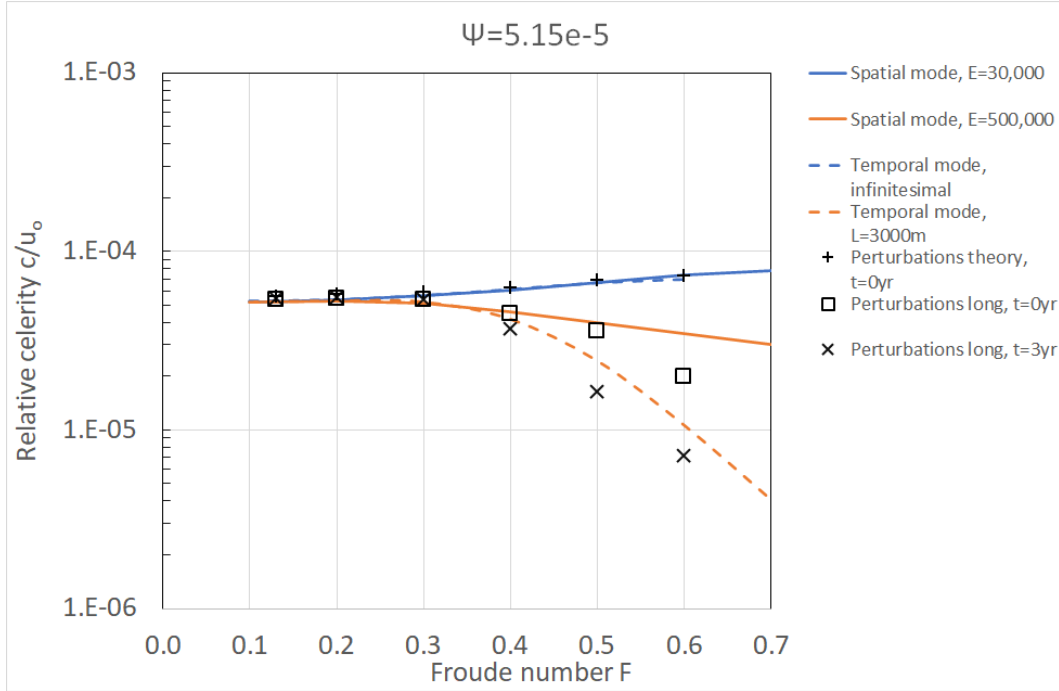


**Figure 11.** Celerities according to the linear stability analysis based on spatial and temporal modes for short and long sediment waves, compared to simulated celerities.

In the domain where analytical models represent the exact solution, they can be used to verify the discretization approach and solution method in numerical models. For

infinitesimal and matching perturbations of flow and river bed (see Section 2.3.4), the analytical approach provides the exact solution of initial propagation and damping of water and sediment waves. This provides valuable validation material for any one-dimensional modelling system, to test whether the processes are correctly implemented, the numerical scheme is appropriate and the numerical parameters and time and space step are properly selected.

For moderate Froude numbers ( $\leq 0.3$ ), the linear stability analysis provides a good first estimate for small perturbations, but underestimates the celerities when sediment waves become larger, and non-linearity and diffusion increase. Figure 12 shows an example of the difference between celerity of a sediment wave from numerical simulations and from the linear stability analysis, based on spatial modes. A value of 1 on the vertical axis means a perfect match. The horizontal axis shows the relative amplitude of the sediment wave, which is defined as the ratio between the amplitude of the sediment wave and the undisturbed water depth. For a sediment wave of 1 meter high and a water depth of 4 meter, the multiplication factor is almost 4 for the initial celerity, and halves after 3 years. Apparently, the multiplication factor shows an almost linear relation with relative wave amplitude for the initial value of the celerity, and flattens this relation for longer simulation times.

These relations could be used as a first indication for the correction factor of the celerity of the linear stability analysis, although it is based on simulations for one Froude number only, and general applicability has not yet been proven. The impact of a flood wave as upstream boundary (see Figure 1) is shown by the open squares in the Figure. The impact is negligible at  $t=0$ . This is understandable as at  $t=0$ , the discharge is equal to the undisturbed discharge and therefore, water depth and flow velocity assume the undisturbed values. After 3 years, the overall celerity increased compared to the initial celerity, due to higher flow velocities and sediment transport rates during flood periods. For realistic flood wave conditions, the appropriate choice of the parameters  $E$ ,  $F$  and  $\Psi$  therefore becomes more diffusive, even more so when flood waves dampen in the downstream direction.

In the Dutch main rivers, morphological changes are ongoing due to historical works and changes of many kinds. New plans are being developed and climate is changing. To assess the impact on river bed morphology, long-term predictions are required. The linear stability analysis allows for a rapid assessment of how fast sediment waves induced by changed boundary conditions or measures travel through the river, and indicate when they may cause problems and require management efforts at downstream locations. The Meuse River is used as an example for assessment of the applicability. In this river, Froude numbers are moderate (on average 0.2 or lower) even during floods for the downstream part, where the bed slope is small and multiple weirs are implemented. In the upstream part of the Dutch Meuse River, referred to as the Border Meuse, slopes are 5 times higher, the river is free flowing and the Froude numbers can take a value of up to 0.5, or locally even higher. This means that the analytically derived sediment wave celerity will be an overestimation in the Border Meuse, because diffusion is high and wave lengths of sediment waves are important (reflected in values of  $E$ ). These wave lengths will change in time. In the downstream part of the Meuse River, sediment waves have a translating character and the linear stability analysis provides a fair estimate of the celerity of low-amplitude sediment waves with various wave lengths.

## 5 Conclusions

A spatial mode linear stability analysis was performed of the one-dimensional St. Venant-Exner equations, with a focus on subcritical flow with Froude numbers  $F$  up to 0.6. The linear stability analysis has yielded explicit relations to estimate celerities and damping lengths of flow and bed perturbations. The results were compared to numer-

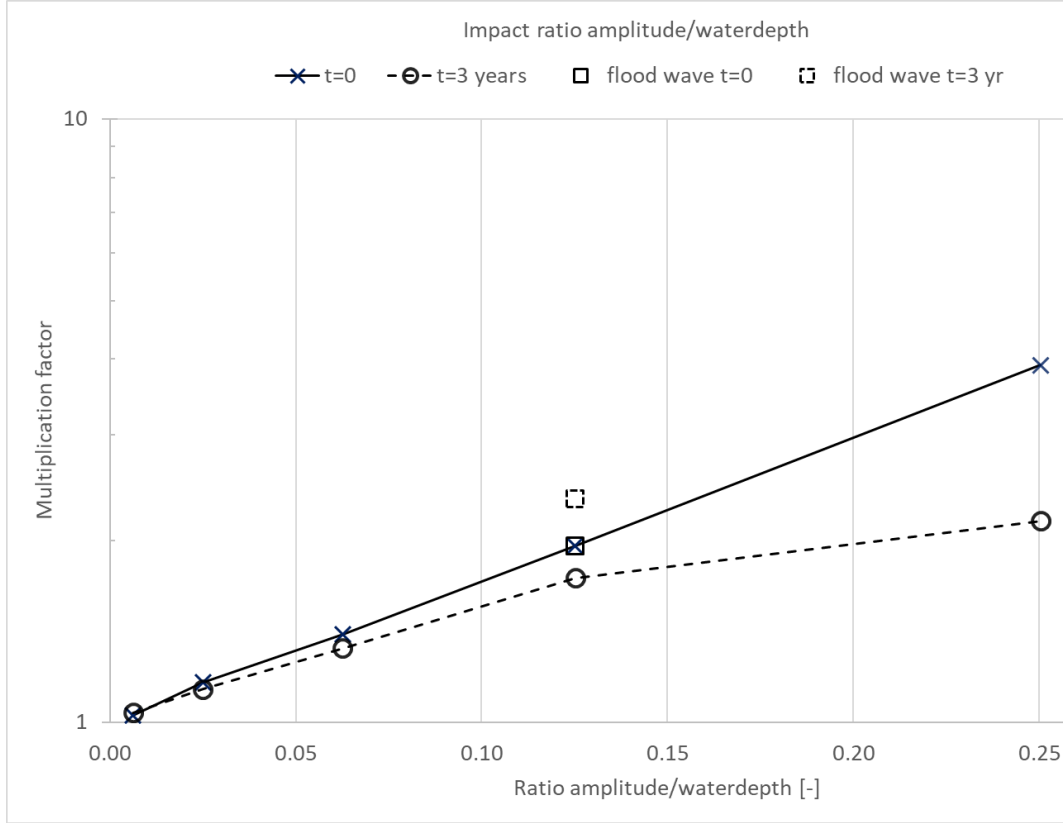


**Figure 12.** Ratio between simulated celerity and celerity from linear stability analysis as a function of ratio of sediment wave amplitude to water depth for  $F=0.2$ .

ical model simulations with ELV, which in turn were verified by several additional model runs with SOBEK-RE. The comparison showed that celerities from the linear stability analysis and numerical results agree well for infinitesimal perturbations at  $t=0$ . Regarding the initial response of these infinitesimal perturbations of the flow and morphology, the linear stability analysis provides excellent information that can be used to validate numerical modelling codes.

For Froude numbers exceeding 0.3, sediment waves show an increasing diffusive character due to which the wave length increases and celerities decrease in time. For these conditions, the linear stability analysis provides an upper limit of the celerity of bed perturbations. When perturbations are higher or longer, attaining dimensions that are significant compared to water depth and the length of the backwater curve, non-linear processes are going to prevail and the diffusive character gains strength. For Froude numbers up to 0.3, the theoretical celerities are a good estimate for perturbations even for longer periods of development, as long as the amplitudes of the sediment waves are smaller than 5% of the depth. When perturbations have larger amplitudes, the linear stability analysis readily underestimates the initial celerity by 50% or more, so a correction factor is required. This correction factor seems to be exponentially dependent on the relative amplitude (ratio amplitude to water depth). Application of a correction would extend the applicability range of the linear stability analysis as rapid assessment tool, but this needs a broader validation.

For higher Froude numbers (0.4 and higher) the diffusive character causes an overestimation of the celerities by the linear stability analysis (based on both spatial and tem-

poral mode analyses) for the longer term. At the same time, non-linearity causes an underestimation by the linear stability analysis. The net impact of diffusion depends on the balance of these two effects and is likely dependent on the value of the Froude number. As an example, the linear stability analysis may be used as rapid assessment tool for sediment waves up to 0.5 m high in the lower part of the River Meuse, referred to as the Sand Meuse. In the upstream steeper part of the river, the Border Meuse, the Froude numbers are higher, diffusion is larger and the linear stability analysis loses predictive power, especially when longer periods of development are subject to study.

## Acknowledgments

This work is a part of the research program Rivers2Morrow (2018-2023). Rivers2Morrow is focusing on a long-term development of the Dutch river system and its response to changing conditions such as river discharges, sea level rise and human interference. Universities, research institutes, NGOs, consultancy companies and government agencies that participate in this program are all working together on knowledge development in order to improve operations, maintenance and policies. Rivers2Morrow is financed by the Directorate-General for Water and Soil and Directorate-General Rijkswaterstaat, both being a part of the Dutch Ministry of Infrastructure and Water Management. HKV and Deltares provide additional support. The authors thank Mart Borsboom of Deltares for his valuable input on numerical aspects of one-dimensional models. Also the discussions with Bart Vermeulen of Wageningen University and Research on the translation and diffusion of bed waves were important for the analyses performed.

## Data availability statement:

In the study numerical simulations have been carried out with the numerical modelling package ELV. ELV is available in the open access repository of the Open Earth Tools managed by Deltares: <https://svn.oss.deltares.nl/repos/openearthtools/trunk/matlab/applications/ELV>. For the simulations we used the version at Revision 16973 from Thursday 17 December, 2020 11:20:54. The input and (reworked) output of the simulations with ELV, presented in the Figures 8, 10 and 11, are available through Barneveld (2021).

## References

- Arkesteijn, L., Blom, A., Czapiga, M. J., Chavarrias, V., & Labeur, R. J. (2019). The quasi-equilibrium longitudinal profile in backwater reaches of the engineered alluvial river: A space-marching method. *Journal of Geophysical Research: Earth Surface*, 124(11), 2542–2560.
- Barneveld, H. (2021). Propagation of bed waves in rivers: Elv simulations, <http://www.hydroshare.org/resource/685314747f4f40f7abad44bb433a96fb>.
- Bélanger, J. B. (1828). *Essai sur la solution numerique de quelques problemes relatifs au mouvement permanent des eaux courantes*. chez Carilian-Goeury, libraire, des corps royaux des ponts et chaussees et . . .
- Carraro, F., Vanzo, D., Caleffi, V., Valiani, A., & Siviglia, A. (2018). Mathematical study of linear morphodynamic acceleration and derivation of the massspeed approach. *Advances in Water Resources*, 117, 40–52.
- Chavarrias, V., Stecca, G., Siviglia, A., & Blom, A. (2019). A regularization strategy for modeling mixed-sediment river morphodynamics. *Advances in Water Resources*, 127, 291–309.
- Church, M., & Ferguson, R. (2015). Morphodynamics: Rivers beyond steady state. *Water Resources Research*, 51(4), 1883–1897.
- Cui, Y., Parker, G., Lisle, T. E., Pizzuto, J. E., & Dodd, A. M. (2005). More on the evolution of bed material waves in alluvial rivers. *Earth Surface Processes and Landforms: The Journal of the British Geomorphological Research Group*, 30(1), 107–114.
- Dade, W. B., & Friend, P. F. (1998). Grain-size, sediment-transport regime, and

- channel slope in alluvial rivers. *The Journal of Geology*, 106(6), 661–676.
- De Vries, M. (1965). Considerations about non-steady bedload transport in open channels. In *Iahr*.
- De Vries, M. (1966). Application of luminophores in sandtransport-studies.
- De Vries, M. (1973). River bed variations-aggradation and degradation. In *Proc. int. seminars on hydr. of alluvial streams, iahr, delft, the netherlands* (pp. 1–10).
- De Vries, M. (1975). A morphological time-scale for rivers. In *WI publication nr. 147, paper presented at the xvith iahr congress, são paulo*.
- Drazin, P. G., & Reid, W. H. (2004). *Hydrodynamic stability*. Cambridge university press.
- Engelund, F., & Hansen, E. (1967). A monograph on sediment transport in alluvial streams. *Teknisk Forlag, Kopenhagen*.
- Grijzen, J., & Vreugdenhil, G. (1976). Numerical representation of flood waves in rivers. *Proc. Int. Symp. Unsteady flow in open channels, Newcastle-upon-Tyne, BHRA Fluid Eng., Cranfield*.
- Ji, Z., De Vriend, H., & Hu, C. (2003). Application of sobek model in the yellow river estuary. In *International conference on estuaries and coasts, hangzhou, china*. retrieved from <http://www.irtces.org/pdf-hekou/114.pdf>.
- Lanzoni, S., Siviglia, A., Frascati, A., & Seminara, G. (2006). Long waves in erodible channels and morphodynamic influence. *Water Resources Research*, 42(6).
- Lesser, G. R., Roelvink, J. v., Van Kester, J., & Stelling, G. (2004). Development and validation of a three-dimensional morphological model. *Coastal engineering*, 51(8-9), 883–915.
- Lisle, T. E., Cui, Y., Parker, G., Pizzuto, J. E., & Dodd, A. M. (2001). The dominance of dispersion in the evolution of bed material waves in gravel-bed rivers. *Earth Surface Processes and Landforms*, 26(13), 1409–1420.
- Lyn, D. A., & Altinakar, M. (2002). St. venant–exner equations for near-critical and transcritical flows. *Journal of Hydraulic Engineering*, 128(6), 579–587.
- Morris, P. H., & Williams, D. J. (1996). Relative celerities of mobile bed flows with finite solids concentrations. *Journal of Hydraulic Engineering*, 122(6), 311–315.
- Ponce, V., & Simons, D. (1977). Shallow wave propagation in open channel flow. *Journal of the Hydraulics Division ASCE, Vol 103, HY12, Proc. Paper 13392, pp1461-1476*.
- Ribberink, J., & Van der Sande, J. (1985). Aggradation in rivers due to overloading-analytical approaches. *Journal of Hydraulic Research*, 23(3), 273–283.
- Sieben, J. (1996). One-dimensional models for mountain-river morphology. *Communications on hydraulic and geotechnical engineering, No. 1996-02*.
- Sieben, J. (1999). A theoretical analysis of discontinuous flow with mobile bed. *Journal of Hydraulic Research*, 37(2), 199–212.
- Sutherland, D. G., Ball, M. H., Hilton, S. J., & Lisle, T. E. (2002). Evolution of a landslide-induced sediment wave in the navarro river, california. *GSA Bulletin*, 114(8), 1036–1048.
- USDA, N. (2007). *National engineering handbook hydrology, chapter 16, hydrographs*. United States Department of Agriculture, Natural Resources Conservation Service.
- Van Vuren, S., Vriend, H. J. D., Ouwerkerk, S., & Kok, M. (2005). Stochastic modelling of the impact of flood protection measures along the river waal in the netherlands. *Natural Hazards*, 36(1), 81–102.
- Vreugdenhil, C. (1982). Numerical effects in models for river morphology. *Engineering applications of computational hydraulics*, 1, 91–110.
- Yossef, M. F., Jagers, H., Van Vuren, S., & Sieben, J. (2008). Innovative techniques in modelling large-scale river morphology. In *River flow 2008, proc. of the intern. conf. on fluvial hydraulics, cesme, izmir, turkey* (pp. 1065–1074).



**Can linear stability analyses predict the development of river bed waves with lengths much larger than the water depth?**

H.J. Barneveld<sup>1,4</sup>, E. Mosselman<sup>2,3</sup>, V. Chavarrías<sup>2</sup>, A.J.F. Hoitink<sup>1</sup>

<sup>1</sup>Wageningen University and Research, Hydrology and Quantitative Water Management Group, Department of Environmental Sciences, Droevendaalsesteeg 3, 6708 PB Wageningen, the Netherlands

<sup>2</sup>Deltares, P.O. Box 177, 2600 MH Delft, the Netherlands

<sup>3</sup>Delft University of Technology, Faculty of Civil Engineering and Geosciences, P.O. Box 5, 2600 AA Delft, the Netherlands

<sup>4</sup>HKV, Botter 11-29, 8232 JN Lelystad, the Netherlands

**Contents of this file**

Text S1 to S4  
Figures S1 to S7  
Tables S1 to S2

**Introduction**

This document contains information on the numerical cases performed with the code ELV (S1), analysis on the impact of another choice of parameters (S2), a comparison between the damping length based on the temporal-mode analysis and spatial-mode analysis (S3) and two field cases to which the results are applied (S4).

---

Corresponding author: Hermjan Barneveld, (hermjan.barneveld@wur.nl)



## Text S1 – Model cases

Table S1 shows the case names for the different simulations presented in Figures 8, 10, 11 and 13 of the manuscript.

**Table S1.** Cases performed in the study

	Cases, see legend in the Figures in the manuscript				
	$\Psi = 5.15 \text{ E-4}$				$\Psi = 2 \text{ E-4}$
	Perturbations theory, t=0yr	Perturbations long, t=0yr	Perturbations long, t=3yr	Perturbations large&long, Qwave, t=3yr	Perturbations theory, t=0yr
Froude number <i>F</i>	<i>Figures 8, 11, 13</i>	<i>Figures 8, 11, 13</i>	<i>Figures 8, 11, 13</i>	<i>Figures 8, 10</i>	<i>Figure 8</i>
0.13	006dXSS2bdyn	006dXSdyn	006dXSdyn	003d25Gdyn	006dXSS3bdyn
0.2	019dXSS2bdyn	019ddyn	019ddyn	013dxGdyn	019dXSS3bdyn
0.3	015dxSmXSS2bdyn	015dxSmdyn	015dxSmdyn	015dxGdyn	015dxSmXSS3dyn
0.4	017dXSS2cdyn	017ddyn	017ddyn	016dGdyn	017dXSS3dyn
0.5	016d5SmXSS2cdyn	016d5Smdyn	016d5Smdyn	016d5Gdyn	016d5SmXSS3dyn
0.6	011dx10aD35XSS2ddyn	018dadyn	018dadyn	011dx10aD35Gdyn	011dx10aD35XSS3dyn

For the assessment of the impact of the choice of the Chézy value on the migration celerity (while keeping the parameters  $F$  and  $\Psi$  equal), the following additional simulations have been performed ( $F=0.2$  and  $\Psi = 5.15\text{E-5}$ ).

- 013DXG2 with  $C=40 \text{ m}^{1/2}/\text{s}$ ,  $D50=0.009 \text{ m}$ ,  $i_b=0.000245$  [-]
- 013DXG2a with  $C=45 \text{ m}^{1/2}/\text{s}$ ,  $D50=0.00633 \text{ m}$ ,  $i_b=0.0001936$  [-].

Results of this analysis can be found in the Section S2 (Impact of the Chézy value).

The input and output of the model runs can be found in the Hydroshare Resource:

Barneveld, H. (2022). Supplementary information propagation of bed waves in rivers: ELV simulations and additional analyses, HydroShare,  
<http://www.hydroshare.org/resource/7842147db84d4265b95fe2872132aa4a>

It contains the following documents:

- The Resource contains following files per case:
- beddev.xlsx - bed level as a function of time and space
- beddev\_dyn\_'name'.xlsx - analysis of beddev.xlsx to assess celerities and generate graphs
- cpu.txt - output cpu time simulation
- input.mat - Matlab input file for ELV
- log.txt - log file simulation
- output.mat - matlab output file ELV

## Text S2 – Impact of the Chézy value

Changing the Chézy value, while maintaining the same values for water depth, velocity, Froude number  $F$  and transport parameter  $\Psi$ , requires changes in the bed slope and  $D_{50}$ , and causes changes in the parameter  $E$ . The linear stability analysis demonstrates the impact of these changes on the relative migration celerity and damping of bed waves. For small Froude numbers ( $<0.3$ ) the impact of changes in bed slope,  $D_{50}$  and  $E$  on the migration celerity is negligible, as can be seen in Figure S1 (for  $F \leq 0.3$  lines overlap).

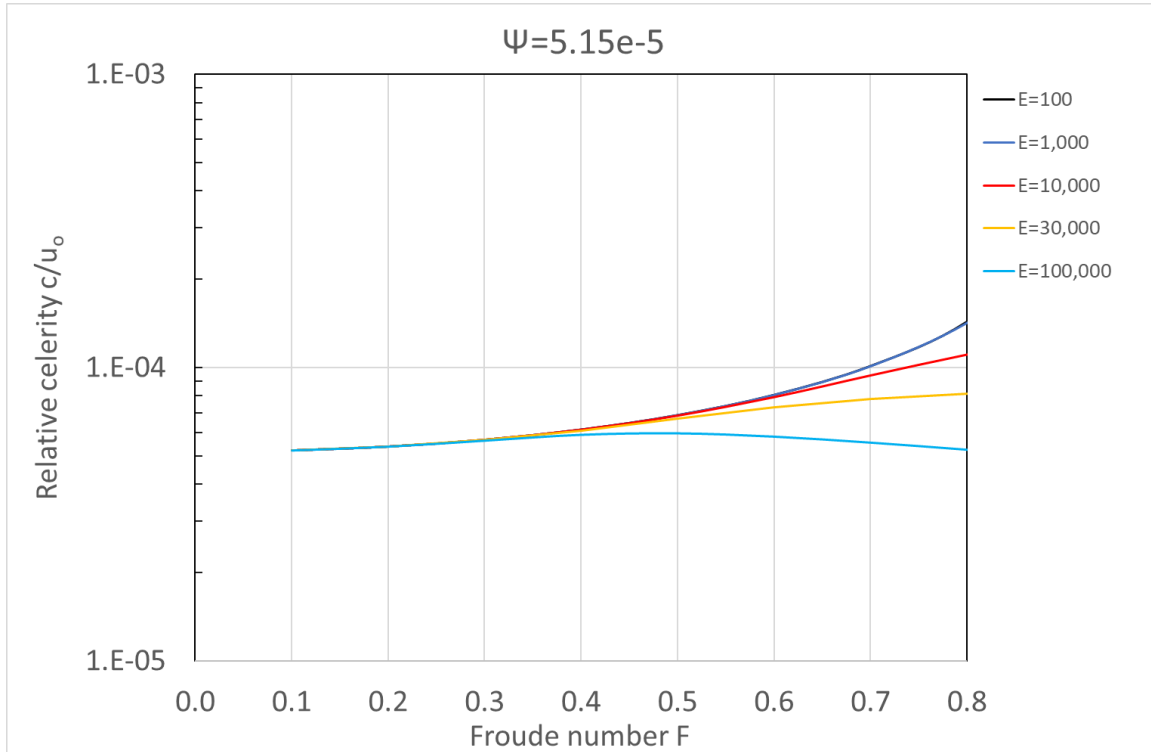


**Figure S1.** Relative celerity of bed waves in the linear stability analysis for  $\Psi = 5.15 \cdot 10^{-5}$  (Figure 3 of manuscript).

We performed additional simulations in which we changed the Chézy value, as well as the values for  $i_b$ , and  $D_{50}$  so as to maintain the same values for  $F$  and  $\Psi$ . Table S2 gives the parameters as chosen, as well as the parameter values that result from these choices.

**Table S2.** Cases for sensitivity analysis for changed conditions for  $C$ ,  $D_{50}$  and  $i_b$ .

parameter	Original simulation Case 013DXG2	Changed condition Case 013DXG2a
$C$ (m <sup>1/2</sup> /s)	40	45
$F$ (-)	0.2	0.2
$\Psi$ (-)	5.15E-5	5.15E-5
$i_b$ (slope)	0.000245	0.0001936
$D_{50}$ (m)	0.009	0.00633

The results of both simulations, in terms of bed level change relative to the original bed slope ( $i_{b,o}$ ), are presented in Figure S2. It can be seen that although the sediment loads appear to differ slightly, and the rates of diffusion in both simulations are somewhat different, the migration celerities (identified at the top of the wave) are almost identical. While keeping  $F$  and  $\psi$  the same, other choices of parameters yield identical results for the migration celerity of the wave, as long as the results are insensitive to changes in parameter  $E$ . This shows that the results of the linear stability analysis are valid, also in case of other parameter choices such as for the Chézy value.

The small differences in damping and diffusion may be due to numerical diffusion in ELV, which could be subject to further research.

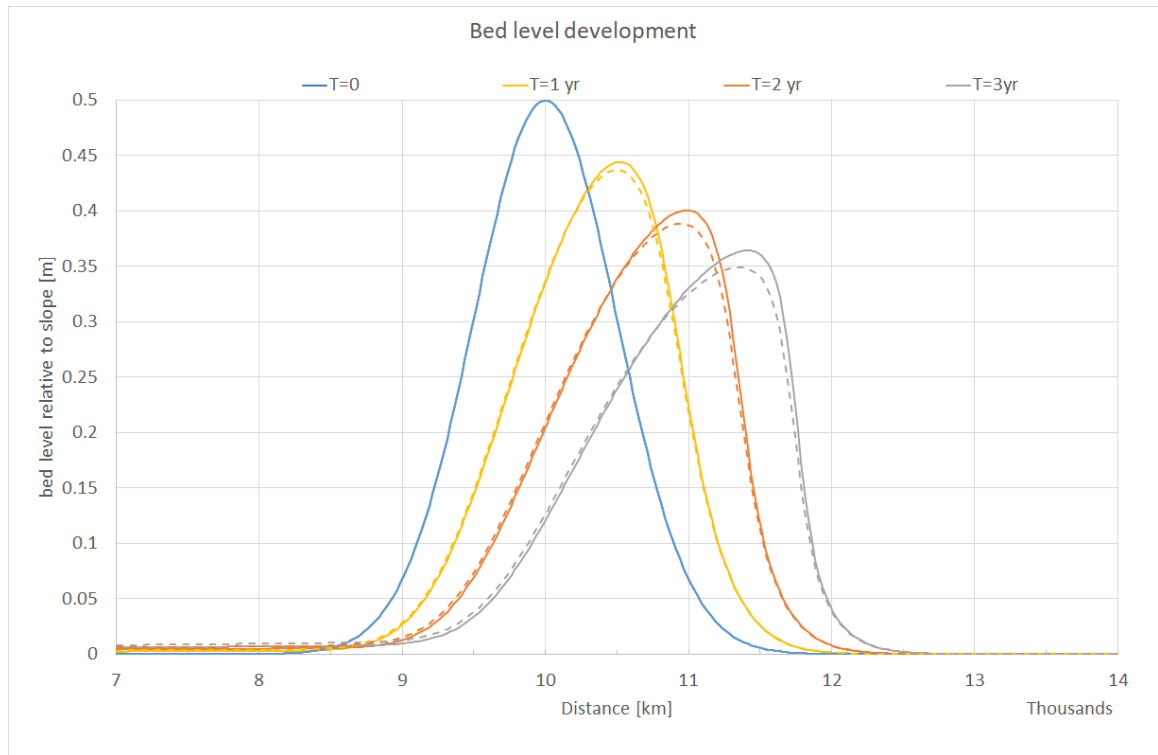


**Figure S2.** Comparison of dynamic of bed wave for alternative choices of  $C$ ,  $D_{50}$  and  $i_b$ . Solid lines: base case 013DXG2; dashed lines: changed conditions case 013DXG2a.

### Text S3 – Damping : Temporal-mode versus Spatial-mode

The damping or relaxation length are calculated in the spatial-mode analysis according to Eq. 16 in the main manuscript. For the temporal-mode analysis, the damping length can be calculated as follows. Suppose the peak of a wave travels with celerity  $c$  over a distance  $X$ . The corresponding travel time is  $T_{Travel} = \frac{X}{c}$ . The damping of the peak during this travel time is given by  $\exp(\omega_i T_{Travel}) = \exp\left(\frac{\omega_i X}{c}\right)$ , with damping factor  $\omega_i$  and celerity  $c$  resulting from the temporal-mode analysis. This damping must also be equal to  $\exp\left(-\frac{X}{L_D}\right)$ , where  $L_D$  denotes the damping length. Hence,  $\exp\left(\frac{\omega_i X}{c}\right) = \exp\left(-\frac{X}{L_D}\right)$ , which implies  $L_D = -\frac{c}{\omega_i}$ .

Plotting this for the damping length  $L_D$  in Figure 11 of the manuscript provides Figure S3.

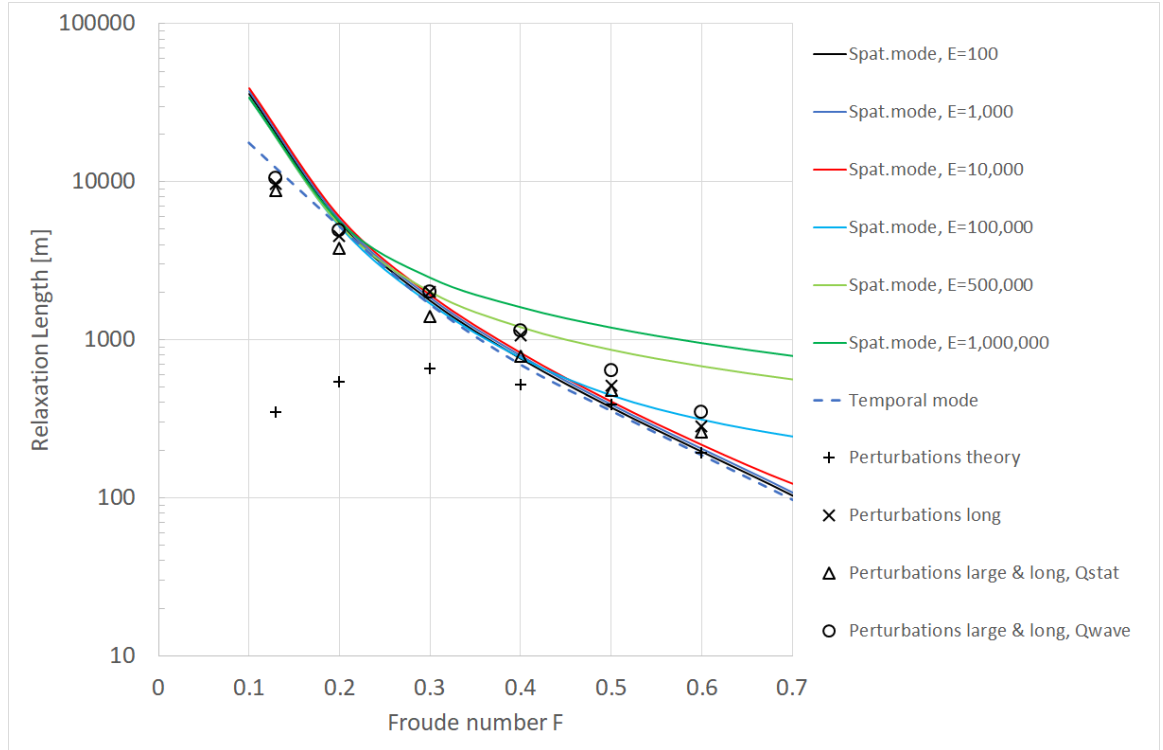


**Figure S3.** Comparison between damping of bed perturbations from linear stability analysis (solid lines for the spatial-mode, dotted line for the temporal-mode) and numerical simulations (markers) for  $\psi = 5.15 \cdot 10^{-5}$ . 'Perturbations theory' represent infinitesimal perturbations with a wave length coupled to the value of  $E$ . For the other simulations, the wave length increased to 3,000 m, while for 'Perturbations large & long, Qwave' the bed wave amplitude increased and a flood wave was applied.

The figure shows that the results from the temporal-mode analysis are close to those from the spatial-mode analysis, for values of the parameter  $E$  up to 1,000.

However, for low values of the Froude number ( $F < 0.2$ ) the damping according to the temporal-mode analysis is somewhat larger (smaller value of  $L_D$ ) than the damping from the spatial-mode analysis, and close to the numerical results for longer bed perturbations ( $x, \Delta, o$ ). For  $F > 0.2$  the value of the parameter  $E$  in the spatial-mode analysis becomes important and the damping-length of the temporal-mode analysis appears to give the lower limit for both spatial-mode analysis results and the numerical results for long bed perturbations.

The comparison to numerical results needs further research, including the impact of numerical diffusion in ELV.

#### **Text S4 – Field cases: Fraser River (Canada) and Waal River (the Netherlands)**

To illustrate the applicability of the linear stability analysis results, two cases with relevant field data for rivers in Canada and the Netherlands are addressed.

Gold mining along the Fraser River between 1858 and 1909 added large amounts of sediment to the river's natural sediment load. Ferguson et al. (2015) and Nelson & Church (2012) reconstructed the impact of the additional sediment supplies on the morphodynamics.

The Waal River in the Netherlands is the main branch of the Rhine delta. The geometry of the river bed of the Waal River has been monitored every two weeks in the period 2005 and 2021. This monitoring material provides detailed information on the migration of bed waves with various wave lengths. Results of these analyses are documented by Gensen & van Denderen (2022).

##### *Fraser River, Canada*

The sediment pulse of place mining on the Fraser River has been analyzed by Ferguson et al. (2015) and Nelson & Church (2012) using observations of the Fraser River channel and numerical modelling. Based on these studies, the following data for the reach between Marguerite and Hope were extracted:

- An average bed slope  $i_0$  of 0.001 (Ferguson et al., 2015);
- A steady dominant discharge of 7,000 m<sup>3</sup>/s operating 15% of the time predicts the total flux of sediment, grain size distribution and net morphological changes for a 20-year period with annual peaks ranging from 6,070 to 12,900 m<sup>3</sup>/s (Ferguson et al., 2015);
- An average channel width of 150 m (Ferguson et al., 2015);
- Froude numbers at mean annual flood of 0.45 at Hope and 0.56 at Marguerite (Nelson & Church, 2012);
- From 456 identified individual mines approximately 58,000,000 m<sup>3</sup> of sediment was excavated, and dumped into the Fraser River between the Cottonwood Canyon (upstream of Marguerite) and Hope (Nelson & Church, 2012);
- An annual travel distance of placer mining sediment ( $L_b$ ) varying between 1 and 6.3 km/yr, with a most likely value of 3.1 km/yr (Nelson & Church, 2012);
- An annual delivery value of 700,000 m<sup>3</sup> of sediment, matching the most likely value of  $L_b$  (Nelson & Church, 2012).

These values were used in the linear stability analyses to assess the migration celerities, both for the spatial mode and the temporal mode approach. In those analyses, a Froude number of 0.5 was adopted as an average. As no information was readily available on flood wave periods (which determine parameter  $E$  in spatial mode analysis) and wave length  $L$  of the bed waves (parameter in temporal mode analysis) these parameters were varied (Figure S4). If the flood duration would be as long as 15% of time over a year (55 days), the parameter  $E$  would be approximately 19,000. Therefore, values of  $E$  larger than 100,000 are unlikely for the Fraser River. A bed wave with a wave

length  $L$  of 25 km or larger would slow down the bed wave to 1 km/yr, or less. Multiple bed waves (with shorter wavelengths, i.e.  $<10$  km) may have moved through the system. Based on the latter assumptions, the migration celerities are in the range 2.25-3.3 km/yr (Figure S4).

The Froude numbers are larger than 0.3-0.4, and therefore, both transition and diffusion may be expected in this part for the Fraser River. Notwithstanding this expected behavior, we conclude that the results of both spatial mode and temporal mode analyses are close to the most likely bed wave migration celerity in this river (3.1 km/yr).

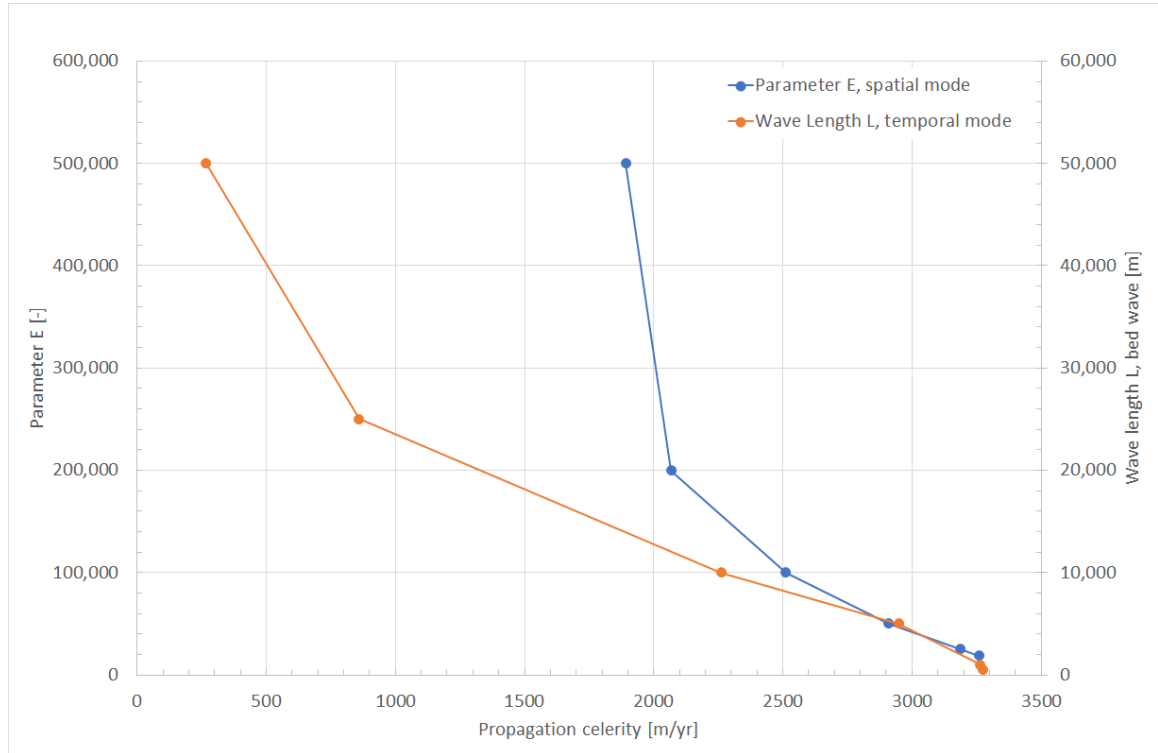


**Figure S4.** Sensitivity analysis on the impact of the parameter  $E$  (spatial mode analysis) and wave length bed wave  $L$  (temporal mode analysis) on the migration celerity of the bed wave. Fixed parameter settings are  $i_0=0.001$ , discharge  $Q=7,000 \text{ m}^3/\text{s}$ , channel width  $W=150 \text{ m}$ , annual sediment load  $S=700,000 \text{ m}^3$  and Froude number  $F=0.5$ .

#### *Waal River, The Netherlands*

The Rhine River enters the Netherlands near the village of Lobith. After approximately 10 km, it bifurcates in the Waal River and the Pannerden Canal. The Waal River flows to the west towards the Rhine-Meuse Delta, in which the large harbor of Rotterdam is situated. The Waal River and Rhine River are of high importance for navigation. The riverbed of these rivers is monitored frequently to assess the navigation depth and to plan dredging activities. In the period 2005-2021, the bed level of the navigation channel has been monitored every two weeks, which means that a large database is available to analyze morphodynamics of the river.

Van Denderen et al. (2022) use these detailed bed level measurements to study the morphological changes on multiple scales using a wavelet transform. A wavelet transform distinguishes and disentangles the bed-level changes on different spatial scales. In this way, the bed level change caused by a local intervention can be separated from larger scale changes. Gensen and Van Denderen (2022) applied this method to filter out bed waves with lengths between 300 m and 4 km. Such bed waves may be initiated by changes in river geometry, combined with flood events. These bed waves subsequently migrate downstream. An example of the result of the wavelet tool can be seen in Figure S5, clearly showing the downstream migration of longer bed waves.

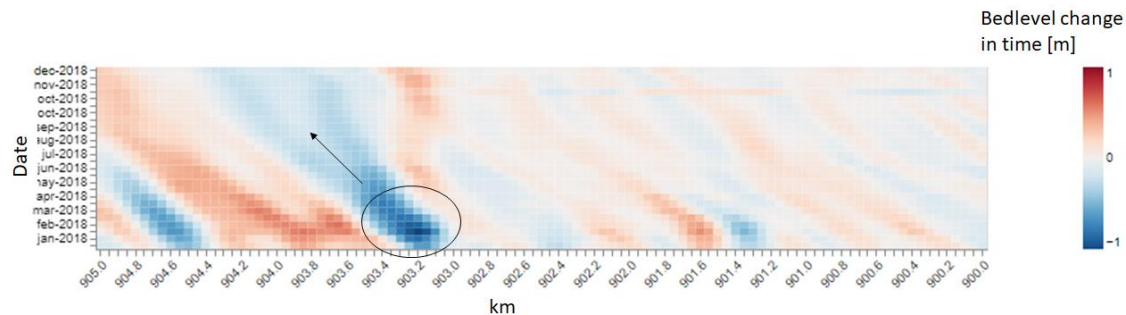


**Figure S5.** Bed level change for part of the Waal River in the year 2018. Clearly, the downstream migration of bed level peaks (red) and troughs (blue) can be distinguished. Water flows from right to left. Source: Van Denderen and Van Hoek (2022).

For comparison of the observed migration celerities, with results of the linear stability analyses, we selected a part of the Waal River which is called the Middle Waal in the reach km 887-915, see Figure S6. This reach is relatively straight and the migration celerities appear to be quite stable in time. For this section, Gensen & Van Denderen (2022) determined an annual travel distance of the bed waves varying between 1.1 and 1.4 km/yr .



**Figure S6.** Rhine and Waal River in the Netherlands. The Rhine enters the Netherlands near Lobith. Downstream from the bifurcation at the Pannerdensche Kop (km 867.5) the Waal River flows to the West. Downstream from the city of Nijmegen, the river is called the Middle-Waal.

Frings et al. (2019) provide an estimate of the annual sediment load for the Waal River of 200,000 m<sup>3</sup> excluding pores ( $\pm 50\%$ ), or 333,333 m<sup>3</sup> ( $\pm 50\%$ ) including pores. Other input parameters for the linear stability analyses are based on the discharge time-series at



Lobith (Figure S7) for the period 2005-2021. This time-series is transformed into representative discharges, specific discharges ( $\text{m}^2/\text{s}$ ), water depths, flow velocities and Froude numbers based on:

1. The distribution of the river discharge at the bifurcation;
2. Water level slope;
3. Average cross-sectional shape containing width of the main section, relative height of the groynes and floodplains;
4. The discharge distribution in the cross-sectional profile (main section, groyne section, floodplain) extracted from numerical model results.

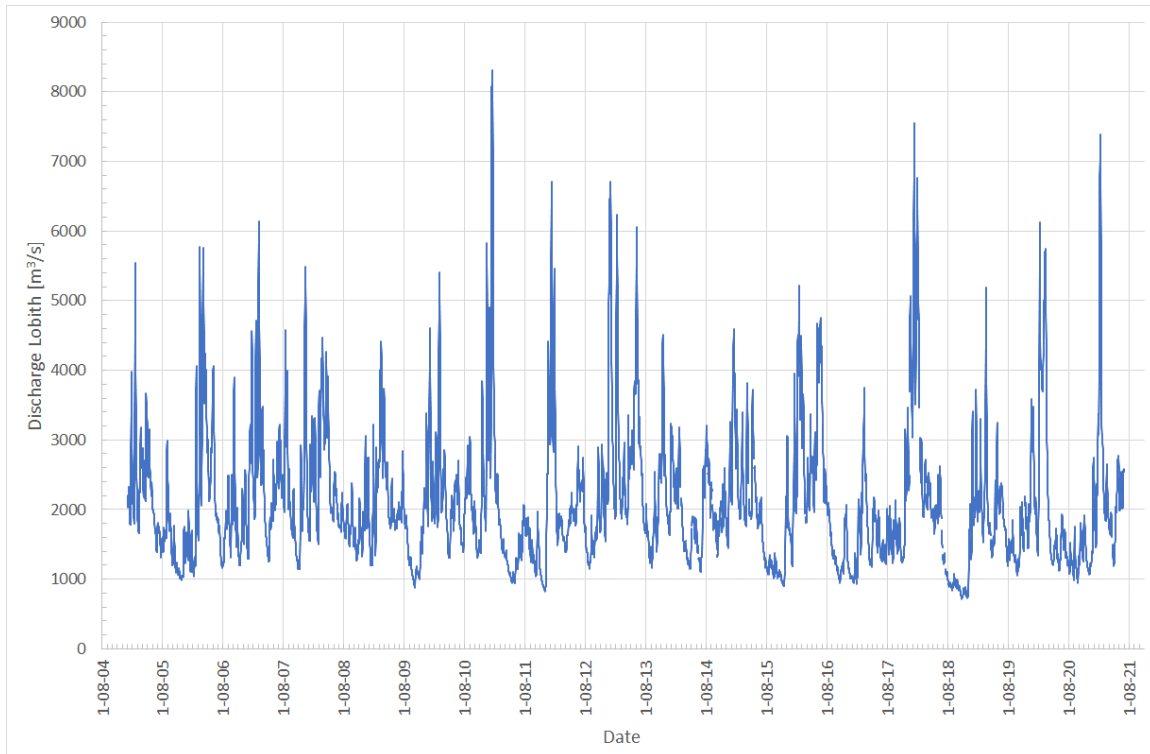


**Figure S7.** Discharge time-series at Lobith for the period January 2005 to July 2021.

This information, combined with river characteristics from Paarlberg & Schippers (2020), yields the following input parameters for the linear stability analyses:

- An average bed slope  $i_o$  of  $1.10^{-4}$ ;
- The average discharge at Lobith in the observation period is approximately  $2,000 \text{ m}^3/\text{s}$ . For the analyses we adopted this discharge level as well as discharge levels of  $1,600 \text{ m}^3/\text{s}$  (overtopping of groynes) and  $3,000 \text{ m}^3/\text{s}$ ;
- With information from Paarlberg & Schippers (2020), for the three discharge levels ( $1,600$ ,  $2,000$  and  $3,000 \text{ m}^3/\text{s}$ ), we determined the corresponding total discharges in the Waal ( $1,268$ ,  $1,461$  and  $2,049 \text{ m}^3/\text{s}$ ), the discharges in the

main river (between the groynes) (1,268, 1,432 respectively 1,900 m<sup>3</sup>/s), and water depth (5, 5,5 and 6,5 m);

- An average channel width of 253 m;
- Froude number of 0.15;
- An annual sediment load of 333,333 m<sup>3</sup>.

Based on this input, the wave celerities in both spatial mode and temporal mode analysis were calculated. We varied the characteristic discharge at Lobith (and the Waal River) and the wave length of the bed wave. Figure 2 in the manuscript shows that for Froude numbers of 0.15, the results are insensitive to the value of the parameter  $E$ .

The results with varying wave length  $L$  of the bed wave (a parameter only in temporal mode) showed insensitivity in the range  $L=300-4000$  m. The discharge at Lobith does exert an influence. When the annual sediment load remains unchanged (333,333 m<sup>3</sup>/yr), the travel distance  $L_b$  is 1,345 m/yr when the discharge at Lobith is 1,600 m<sup>3</sup>/s. For discharges at Lobith equal to 2,000 m<sup>3</sup>/s (mean discharge) and 3,000 m<sup>3</sup>/s,  $L_b$  reduces to 1,222 and 1,035 m/yr, respectively. Differences in results of the spatial mode and temporal mode are negligible.

Choosing an average discharge (2,000 m<sup>3</sup>/s) apparently provides a good approximation of the observed annual travel distance of 1.1 and 1.4 km/yr. Adopting low (1,600 m<sup>3</sup>/s) or high (3,000 m<sup>3</sup>/s) estimates of the discharge at Lobith yield bed wave celerities matching the observed values, but at the borders of the band width of the observations. It should be realized that the annual sediment load was identical for the three discharge values (333,333 m<sup>3</sup>/yr). It can be concluded that adopting a correct value for the annual sediment load is more important than the selected value of the discharge, as the celerity appears to be linearly dependent on the sediment load.

## REFERENCES

Ferguson, R. I., M. Church, C. D. Rennie, and J. G. Venditti (2015), Reconstructing a sediment pulse: Modeling the effect of placer mining on Fraser River, Canada, J. Geophys. Res. Earth Surf., 120, 1436–1454, doi:10.1002/2015JF003491.

Frings, R. M., G. Hillebrand, N. Gehres, K. Banhold, S. Schriever, and T. Hoffmann (2019), From source to mouth: Basin-scale morphodynamics of the Rhine River, Earth-science reviews 196: 102830.

Gensen M. and R.P. van Denderen (2012), Propagation celerity bed disturbances using bed level soundings Rhine and Waal, in Dutch: "Loopsnelheid bodemverstoringen - Op basis van vaargeulpeilingen Bovenrijn/Waal", Report HKV, PR4597.10, March 2022.

Nelson A.D. and M. Church (2012), Placer mining along the Fraser River, British Columbia: The geomorphic impact, Geological Society of America Bulletin; July/August 2012; v. 124; no. 7/8; p. 1212–1228; doi: 10.1130/B30575.1

Paarlberg A. and M. Schippers (2020), Inverse modelling equilibrium effect of measures on main river bed: deriving dimensions of measures, In Dutch: "Inverse modellering evenwichtseffect maatregelen op zomerbedbodem: afleiden dimensies van maatregelen", 22 January 2020.

Van Denderen R. P. and M. van Hoek (2022), Wavelet application, Help documentation, in Dutch: "Waveletapplicatie, Helpdocumentatie", Report HKV, PR4591.10, March 2022.

Van Denderen R. P., E. Kater, L. H. Jans, and R.M. Schielen (2022), Disentangling changes in the river bed profile: The morphological impact of river interventions in a managed river. Geomorphology, 408, 108244.